



Microfluidic devices for cell cultivation and proliferation

Masoomeh Tehranirokh,^{1,a)} Abbas Z. Kouzani,¹ Paul S. Francis,² and Jagat R. Kanwar³

¹*School of Engineering, Deakin University, Geelong, Victoria 3216, Australia*

²*School of Life and Environmental Sciences, Deakin University, Geelong, Victoria 3216, Australia*

³*Nanomedicine-Laboratory of Immunology and Molecular Biomedical Research (NLIMBR), School of Medicine (SoM), Molecular and Medical Research (MMR) Strategic Research Centre, Faculty of Health, Deakin University, Geelong, Victoria 3216, Australia*

(Received 11 June 2013; accepted 24 September 2013; published online 29 October 2013)

Microfluidic technology provides precise, controlled-environment, cost-effective, compact, integrated, and high-throughput microsystems that are promising substitutes for conventional biological laboratory methods. In recent years, microfluidic cell culture devices have been used for applications such as tissue engineering, diagnostics, drug screening, immunology, cancer studies, stem cell proliferation and differentiation, and neurite guidance. Microfluidic technology allows dynamic cell culture in microperfusion systems to deliver continuous nutrient supplies for long term cell culture. It offers many opportunities to mimic the cell-cell and cell-extracellular matrix interactions of tissues by creating gradient concentrations of biochemical signals such as growth factors, chemokines, and hormones. Other applications of cell cultivation in microfluidic systems include high resolution cell patterning on a modified substrate with adhesive patterns and the reconstruction of complicated tissue architectures. In this review, recent advances in microfluidic platforms for cell culturing and proliferation, for both simple monolayer (2D) cell seeding processes and 3D configurations as accurate models of *in vivo* conditions, are examined. © 2013 AIP Publishing LLC. [<http://dx.doi.org/10.1063/1.4826935>]

I. INTRODUCTION

In recent years, microfluidic devices have been increasingly utilised in a wide variety of fields,¹⁻³ where the small sample and reagent consumption and controlled fluid behaviour (characterised by laminar flow, diffusion mixing and rapid energy dissipation) have been exploited to create cost-effective, compact, integrated, and high-throughput systems that were not possible using traditional macroscale techniques. Moreover, with channel and chamber dimensions commensurate with biological cells and tissue, microfluidic devices can provide precisely controlled environments for the study of cell-cell and cell-extracellular matrix (ECM) interactions, soluble factors and mechanical forces, as well as single-cell handling, with real-time observation and analysis.⁴⁻⁶ Cells can be cultured on microfluidic devices, with channels enabling convenient diffusion of substrates, nutrients, and reagents delivered by continuous perfusion systems. The application of forces such as dielectrophoresis (DEP), optic and magnetic forces, enable the concentration, separation, and sorting of cells.⁷⁻¹⁰

This emerging technology has great potential for stem cell research, where porous artificial ECM scaffolds can be created to accommodate cell differentiation and tissue regeneration under physiologically relevant conditions. For this purpose, biocompatible materials that promote cell adhesion, growth, and differentiation and minimise body reaction and inflammation are most desirable.^{11,12} By surface coating with ECM proteins such as collagen, fibronectin, and laminin, biomimetic scaffolds

^{a)}Author to whom correspondence should be addressed. Electronic mail: mtehrani@deakin.edu.au. Telephone: +61352272405

with superior effectiveness for cell seeding and distribution can be attained.¹³ Uniform cell distribution inside the scaffolds is an important issue, which has been addressed by approaches such as surface acoustic wave actuations with an amplitude of a few tens of nanometres.¹⁴

There are numerous excellent reviews of microfluidic cell culture platforms,^{15–19} stem cell studies in microenvironments,^{20–24} the design of microfluidic devices for biological research,^{25–28} the potential of microfluidic chips for investigating neurological diseases,^{29,30} and biomolecular gradients in cell culture systems.^{31,32} In this paper, recent innovations in microfluidic platforms for cell patterning, culturing, and proliferation are examined, with discussion divided into: microperfusion and cell cultivation (first for different cell lines and then with particular focus on stem cells), gradient-generator microfluidic devices that provide cell culture microenvironments in which cells are exposed to a gradient of biomolecular cues and finally, cell patterning and positioning prior to cultivation.

II. MICRO PERFUSION AND CELL CULTURE

Traditional macroscale cell culture environments consume large cell numbers, cell medium, and other resources needed for assays. Through miniaturization, homogenous culture environments with low chemical gradients can be established.^{1–3} Culturing cells in microfluidic devices combined with microperfusion systems enables the delivery of continuous nutrient supplies and waste removal while keeping the system sterile. Microscale cell culture platforms have been used to study many biological processes and responses, including stem-cell growth, proliferation, and differentiation.^{20–24} Cells can be cultured using simple monolayer (2D) cell seeding processes or in 3D configurations, more akin to *in vivo* conditions. In this section, we initially review the cultivation of various cell lines within microfluidic devices utilising 2D and 3D approaches, and then focus on stem cell applications. In each part, integration and multiplexing for real-life applications and large-scale experimentation are presented separately.

A. Cell cultivation and perfusion

1. 2D vs 3D cell culture

Cell cultivation within 2D platforms is appropriate to control large quantities of cells, real-time analysis of their behaviour, and fluorescence detection methods.¹⁶ 2D cell culture in microfluidic devices have been widely used for investigation of cellular responses and viability. Microfluidic-based cell culture systems have been used for both static and continuous-perfusion for 2D cell culture in a sustainable microenvironment. In 2D cell-culture systems, cells are cultured as a monolayer on a surface and do not mimic the morphology that the cells have in body, and shear stress of growth factors and even oxygen are harmful for cell viability.^{1,17,33} In 2D culture environments, cells lose their phenotypes while a 3D culture offers an environment like real tissue, and cells grow more similarly to their *in vivo* phenotypes with regulated cell-cell and cell-matrix interactions. Homotypic or heterotypic interactions with neighbouring cells are important to explore cell response and behaviour. 2D culture conditions are unable to mimic the biological complexity of cells in body except for specific cells like endothelial cells.²⁶ 2D culture of epithelial cells on flat substrates can mimic the *in vivo* responses to drugs and certain toxins in toxicology assays, but most cells need signals from a 3D environment for relevant physiological behaviour and response.^{34,35} Biomaterial scaffolds are capable of providing environments for cell attachment and tissue growth.^{36,37} Microfluidic devices offer controlled environments for regulatory signals such as cytokines and physical factors like hydrodynamic shear. 3D cell culture offers constructing functional grafts for implantation, tissue repairing, disease studies, stem cells behaviour investigation, and developmental processes in controllable 3D forms.²⁰

The diverse scope of microfluidics-based research in this area is evident from a survey of recent literature, which includes new approaches to precisely control fluid movement,^{38–40} mimic biological functions,^{40,41} study cell behaviour/interactions,^{42–45} and undertake high-throughput cell culture and analysis.^{39,46,47} 3D cell cultures have been developed using gels as an extracellular matrix^{48–52} or microstructural components to shape the 3D system.^{53,54}

2. Mimicking biological functions

To simulate the functions, mechanics and physiological response of an entire organ or organs systems, microfluidic devices such as lung-on-a-chip,⁵⁵ Heart-on-a-chip,⁵⁶ and artery-on-a-chip⁵⁷ have been developed. Microfluidic devices for cultivation of cells as a liver model in 2D^{40,41,58} and 3D^{53,54} have been fabricated. To maintain temporary hepatic support for patients with liver malfunction, bioartificial liver (BAL) devices with long time survival of hepatocytes have been developed.⁵⁸ Designing the flow environment with some microstructures to minimise shear stress on cells, improves cells growth and survival significantly. For the development of a bioartificial liver, Park *et al.*⁴¹ designed a radial-flow bioreactor to protect seeded hepatocytes from the damaging shear stress of the convective metabolic exchange. The bioreactor comprised a stack of circular glass substrates with concentric microgrooves in a polycarbonate housing (Fig. 1(A)). All microgrooves were 50 μm deep with 50 μm spacing, but the groove width was varied according to location (50 μm for radial distances 2.5–12 mm, 100 μm for 12–17 mm, and 200 μm for 17–25 mm). Plastic spacers created 100 μm channels between the glass substrates. A peristaltic pump was used to circulate the culture medium between the reservoir, oxygenator and bioreactor. At a volumetric flow rate of 18 ml/min (0.833 ml/min per channel), the shear stress was still below the critical value of 0.33 dyn/cm². After 36 h perfusion, the viability of hepatocytes was found to be 95%, 95%, and 94% on substrates with microgrooves at radial distances of 20 mm, 12 mm, and 5 mm, compared to 98%, 28%, and 0% on substrates without microgrooves, where shear stresses of ~ 0.5 to 5 dyn/cm² were encountered. Based on hepatic organ architecture and physiological data from human microvasculature, Carraro *et al.*⁴⁰ designed a two-layer microfluidic device that contained a network of channels mimicking blood vessels in one layer and a parenchymal chamber in the other. The layers were separated by a nanoporous polycarbonate membrane that allowed the transfer of metabolites, but protected the hepatocytes from deleterious shear stress. The width of the main inlet and outlet channels was 2650 μm , which gradually branched and decreased to 35 μm , within hepatic sinusoid-like structures. The depth of the channels and chamber was 100 μm . Medium was injected into the system by a syringe pump at a flow rate of 0.5 ml/h. The device maintained long-term (14 day) liver cell viability, proliferation, and hepatic function. Cell number and viability were significantly enhanced by coating the polycarbonate membrane with collagen to serve as an extracellular matrix. To study the cultivation of the hepatocarcinoma cell line HepG2/C3A, as a liver cell model in 3D form, Baudoin *et al.*⁵⁴ studied the cultivation of the hepatocarcinoma cell line HepG2/C3A in a microfluidic device. The device consisted of two PDMS layers. Microstructures (for enhancing 3D cell cultivation) on the bottom layer consisted of series of microchambers (520 $\mu\text{m} \times 520 \mu\text{m} \times 100 \mu\text{m}$) and microchannels (720 $\mu\text{m} \times 220 \mu\text{m} \times 100 \mu\text{m}$) placed in a 200 μm deep cell culture chamber with a geometry suitable for a uniform flow (Fig. 1(B)). The inlet and outlet were located on the above PDMS layer and the total volume of the cell culture chamber was 40 μl (area of 2 cm²). The metabolic activity of cells at different flow rates of medium (0, 10 and 25 $\mu\text{l}/\text{min}$) was investigated, and the device was tested for toxicological analysis. Without using biological or synthetic matrices, Goral *et al.*⁵³ fabricated a perfusion-based microfluidic device for 3D cultivation of primary human hepatocyte cells. The device consisted of a cell culture chamber (100 μm width), two side microchannels and a series of retention micropillars placed around the chamber (Fig. 1(C)). The cell culture chamber was patterned with microstructures to control the hepatocyte polarity by reducing cell spreading and cell-surface interactions. Cell culture media was introduced at 5 $\mu\text{l}/\text{h}$ into the side microchannels by syringe pump. After 2 weeks of perfusion, high viability of primary human hepatocytes was observed (>90%) and hepatocytes adhered firmly together to shape 3D cord-like structures. A concentration gradient in the cell culture area was created by introducing two different fluids into the inlets of the side channels.

3. Cells behaviour/interactions

Dynamic cell co-cultures in multicompartamental bioreactors allow the study of several cell lines that share the same environment. Ciofani *et al.*⁴² developed a dynamic two-compartment

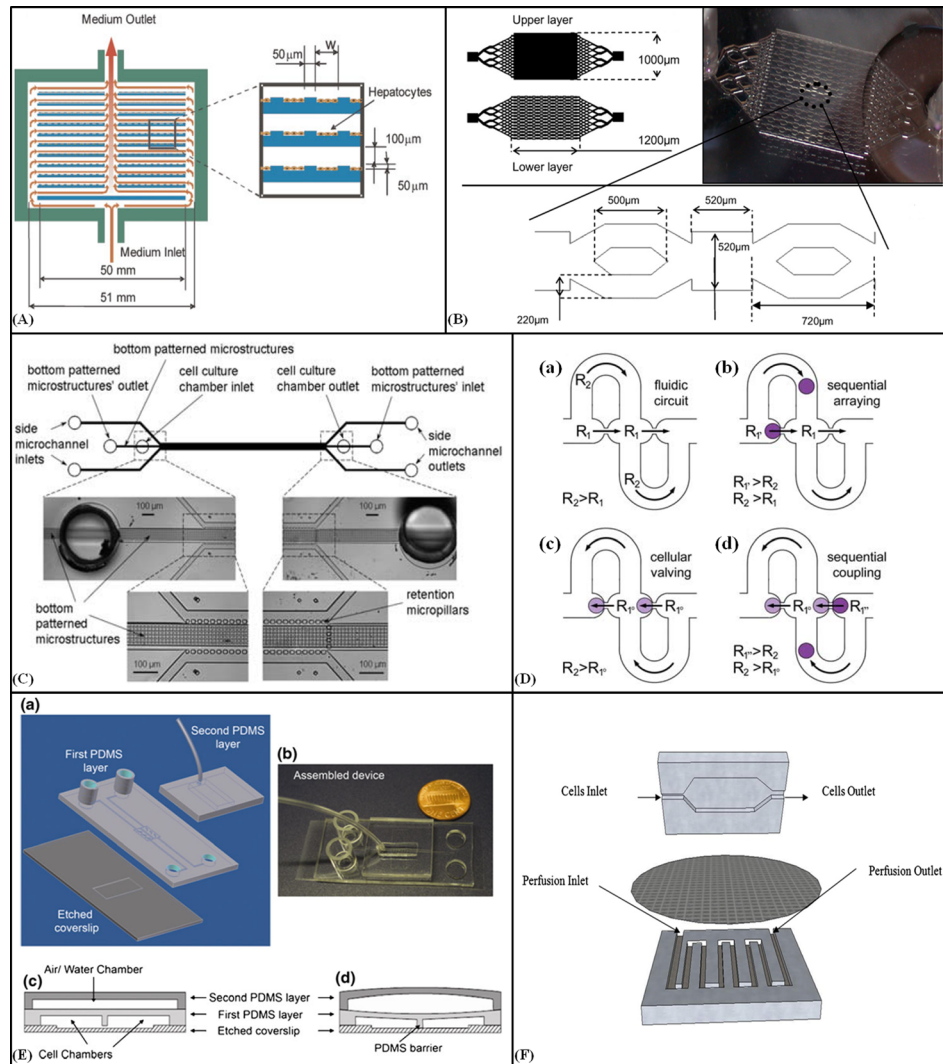


FIG. 1. 2D and 3D cell culture. (A) Schematic diagram of the radial-flow bioreactor with microgrooves for 2D culture of Hepatocytes. Reprinted with permission from Park *et al.*, *Biotechnol. Bioeng.* **99**, 455–467 (2008). Copyright 2007 Wiley Periodicals, Inc., John Wiley and Sons. (B) Design of the microfluidic bioreactor for hepatocarcinoma cultivation in 3D cell layers. Reprinted with permission from Baudoin *et al.*, *Biochem. Eng. J.* **53**, 172–181 (2011). Copyright 2011 Elsevier. (C) Schematic diagram of perfusion-based microfluidic device with a series of retention micropillars for 3D culture. Reproduced by permission from Goral *et al.*, *Lab Chip* **10**, 3380–3386 (2010). Copyright 2010 by The Royal Society of Chemistry. (D) The cellular valving principle for cell pairing. (a) A spherical channel with a series of apertures. (b) Cell trapping. (c) Diverting the streamline. (d) Flow reversal used to introduce a second spherical cell type and sequential single cell pairing. Reproduced by permission from Frimat *et al.*, *Lab Chip* **11**, 231–237 (2011). Copyright 2011 by The Royal Society of Chemistry. (E) (a) A schematic of the microfluidic cell co-culture platforms to study cell-cell interactions for 2D and 3D culture. (b) The fabricated device. (c) and (d) Diagrams of the barrier valve working mechanism. Reprinted with permission from Gao *et al.*, *Biomed. Microdevices* **13**(3), 539–548 (2011). Copyright 2011 Springer Science+Business Media. (F) Schematic of the microfluidic 2D cell culture device with a sandwiched PC membrane between culture chamber and perfusion chamber. Reprinted with permission Shah *et al.*, *Sens. Actuators, B* **156**, 1002–1008 (2011). Copyright 2011 Elsevier.

cell culture device to investigate the interactions between different cell lines and their reactions to external stimuli. Parallel interconnected inlet and outlet channels distributed the flow equally between the two chambers. The depth of the chambers and the channels were different (5 mm and 2 mm, respectively), so that the cells were not subjected to direct flow from the inlet. The length and width of each chamber was 15×10 mm, providing a similar area to that in a 24-well plate. Kidney Crandell feline fibroblast (CrFK) and immortalised mouse hippocampal (HN9.10e) cell lines were seeded on 10 mm diameter glass dishes and after cell adhesion, the

glasses were positioned inside the chambers, and a flow rate of 24 $\mu\text{l}/\text{min}$ of nutrient was maintained by a peristaltic pump. Simulations showed that for the dynamic state, the oxygen concentration and flux were higher than the static condition. Experiments for both cell lines showed sufficient growth rates and metabolic activity. Micro-scale environments compatible with cellular and sub-cellular sizes are suitable for single cell–cell contact investigations. Frimat *et al.*⁴⁵ presented a serpentine microfluidic array with a series of apertures for single cell co-culture by cellular valving. The apertures created a linear path with a resistance lower than the serpentine flow path (Fig. 1(D)). At first, a cell was transported within the linear flow path and trapped at the first gap. The blocked linear path with increased fluidic resistance diverted the streamlines. A second cell type was trapped with the reversed flow and placed in contact with the other cell for co-culture. The adhered and flattened cells (flattened morphology of cells after adhesion), acted as a valve in the open state to restore the differential fluidic resistance. Both heterotypic and homotypic single cell co-cultures in an array format for high throughput screening were developed. Human SW480 epithelial cells, MCF-7 epithelial-like breast cancer cells, and HT29 colon carcinoma cells were utilised. Hydrostatic pressure-driven delivery was used to introduce the media (5 $\mu\text{m}/\text{s}$) and cells (50 $\mu\text{m}/\text{s}$). The simulated shear stress on cells was 0.7 dyn cm^{-2} during cell loading and 0.07 dyn cm^{-2} during co-culture perfusion. Plasma stencilling in the linear path was applied to detain the cells within the traps. Larger trap sizes allowed the highest levels of cell coupling. For 3D cell co-culture, Gao *et al.*⁵⁰ reported a simple microfluidic cell co-culture platform with a pressure-controlled valve barrier between two cell populations for real-time imaging of interactions, in both 2D and 3D cell cultures (Fig. 1(E)). The device consisted of two PDMS layers; the first contained the inlet and exit wells and microchannels, and two microchambers (L: 6 mm, W: 0.7 mm, H: 0.06 mm) separated by a thin PDMS valve barrier (W: 100 μm). A pressure chamber in the second layer controlled the height of the barrier, enabling connection or isolation of the two cell populations. A continuous flow of media was achieved by the pressure difference between the loading reservoirs and the waste wells. The device was used for dynamic observation of synapse formation in central nervous system neurons and tumour cell-endothelial cell cross-migration. The cells were healthy over the culture period up to 3 weeks. Utilising an Agarose-coupled valve barrier enabled the study of cell-cell interactions through soluble factors alone. 3D cell co-culture (human mammary epithelial cells and normal human dermal fibroblasts) was demonstrated by loading a mixture of cells and Matrigel as an extracellular matrix.

Shah *et al.*⁵⁹ fabricated a user friendly and low cost microfluidic cell culture device with diffusion-based perfusion of cells for non-adherent cell cultures. The device consisted of a culture chamber (250 μm deep) and a perfusion chamber (H: 300 μm , W: 500 μm) divided by a sandwiched PC membrane (5 μm pore size) as a scaffold for cell culture (Fig. 1(F)). The perfusion chamber had a meandering channel for uniform diffusion of media (75 $\mu\text{l}/\text{h}$) in the culture chamber and bubble removal. The device was used for cytogenetic sample preparation for culturing whole blood for expansion and arrest of T-lymphocytes, and then fixing the cells for subsequent analysis. For long term dermal fibroblast cell culture, Marimuthu and Kim fabricated and tested a pumpless energy-efficient microfluidic perfusion cell culture chip.⁶⁰ Their device worked by gravity-driven flow by means of an intravenous (IV) infusion set, maintaining the steady flow rate from 0.1 to 10 ml/min. They examined the device for dermal fibroblast cell culture for 3 weeks and showed that 1 and 5 ml/min flow rates were appropriate shear flows for cultivation.

4. Integration and multiplexing

a. Integrated cell culture systems. Complex microfluidic cellular assays and studies would benefit from accurate computer-controlled methods and integrated devices with pumps, valves and mixers to control fluid flows inside fluidic networks. PDMS as the bulk material in microfluidics allows the incorporation of elements to develop integrated and programmable devices for various applications. These systems offer high-throughput cell-based screening assays and furthermore the devices are not required to be redesigned for new microfluidic applications. In

an elegant, integrated approach to control fluid flow inside a microchannel network, Gu *et al.*⁶¹ utilised computer-controlled, piezoelectric movable pins located on a refreshable Braille display. The 0.9 mm pins were employed as valves through localised deformations (0.2 N vertical force) of a thin PDMS sheet used to seal the channels, and three sequential valves were used as a peristaltic pump. With this device, the C2C12 mouse myoblast cell line was seeded, compartmentalised and maintained for 3 weeks under perfusion. At 15 nl/min perfusion, cells proliferated and migrated against the direction of fluid flow, while higher flow rates led to faster outgrowth. Changing the flow direction altered the direction of cellular outgrowth.

A programmable microfluidic device with 64 nodes, controlled by 114 independently addressable valves was developed by Fidalgo and Maerkl³⁸ for automated biological applications such as immunoassay and cell culture. Each node was enclosed by up to four valves allowing many possible interconnections and channel structures. A multiplexer was incorporated to reduce the number of external inputs to 15. By pressurising all valves, each of the 64 network nodes was converted into a 300 pl reaction vessel. Opening a series of valves between the entrance and exit created a route through the network to control the introduced solutions at any given time, which could be undertaken within 1.6 to several seconds, depending on the complexity of the path. The potential of this device for cell culture was demonstrated with a multiplexed yeast culture experiment. For high-throughput cell-based screening assays, Wang *et al.*³⁹ fabricated a microfluidic array of individually addressable cell culture chambers controlled by pneumatic valves. The device consisted of two layers; a fluidic layer containing the channels and chambers (both 18 μm depth) for delivering and culturing cells, and a “control” layer containing the valve channels, which isolated the culture chambers from the fluidic channels when a pressure of 30 psi was applied. Chinese hamster ovary cells (CHO-K1) were introduced into the fibronectin-coated array using a syringe pump (1.5 $\mu\text{l}/\text{min}$). After seeding, pipette tips filled with medium were inserted into the inlets to supply continuous gravity-driven perfusion. Cellular responses with different reagents in designated chambers were successfully examined. Liu *et al.*⁴³ introduced an integrated microfluidic device for efficient study of microenvironmental cell interactions (Fig. 2(A)). This four-layer device was composed of microchannels (W: 200 μm , H: 35 μm), four chambers (D: 600 μm , H: 35 μm), control channels (W: 25–100 μm , H: 25 μm) controlled by external solenoid valves, two multiplexers and nine inlets and one outlet for cell loading and solutions. Different cell lines (human hepatocellular carcinoma cells (HepG2) and mouse embryonic fibroblasts, MEFs (NIH 3T3)) were seeded on collagen coated chambers kept from cross contamination by valves. A medium flow rate of 0.3 $\mu\text{l}/\text{min}$ was used, which caused a maximum shear stress of 0.7 dyn/cm^2 on the cells. The results showed the passive role of NIH 3T3 fibroblasts in response to the signals and variable behaviours of carcinoma cells under various environmental stimulations.

Lee *et al.*⁴⁴ fabricated a rigid PDMS device for automated microscale continuous cell-culture investigations. Eight inputs for media were connected to on-chip reservoirs (35 μl) to decrease pressure variations (Fig. 2(B)). An integrated peristaltic pump (consisting of three valves) transferred the media to three interconnected growth chamber sections containing PDMS membranes. Each section acted as a valve that could inflate to fill with 500 μl liquid. Actuation of the three membrane valves in a circular pattern produced peristaltic mixing of the 1 ml working volume. A pass-through channel enabled switching between pumping to the growth chamber and waste output. Fluid pressurization, movement, and isolation were controlled with a series of blocking valves (see B1-B4, P1, and P2 in Fig. 2(B)). Three weeks continuous culture of *Escherichia coli* was performed, and the device showed precise flow, temperature, cell density, and pH control, with high oxygen transfer rate (0.025 s^{-1}) and fast mixing (2 s).

b. Digital microfluidics (DMF) for multiplexing. DMF is a technique for manipulation of picolitre to microlitre-sized droplets, actively (electrostatic) or passively (surface tension) on a surface containing an array of electrodes. By using this method, all the steps required for cell culture from cell seeding to reagent dispensing can be accomplished for multiplexed assays. Furthermore, this fluid-handling technique is compatible with conventional high-throughput screening techniques. Barbulovic-Nad *et al.*⁶² reported the first application of digital

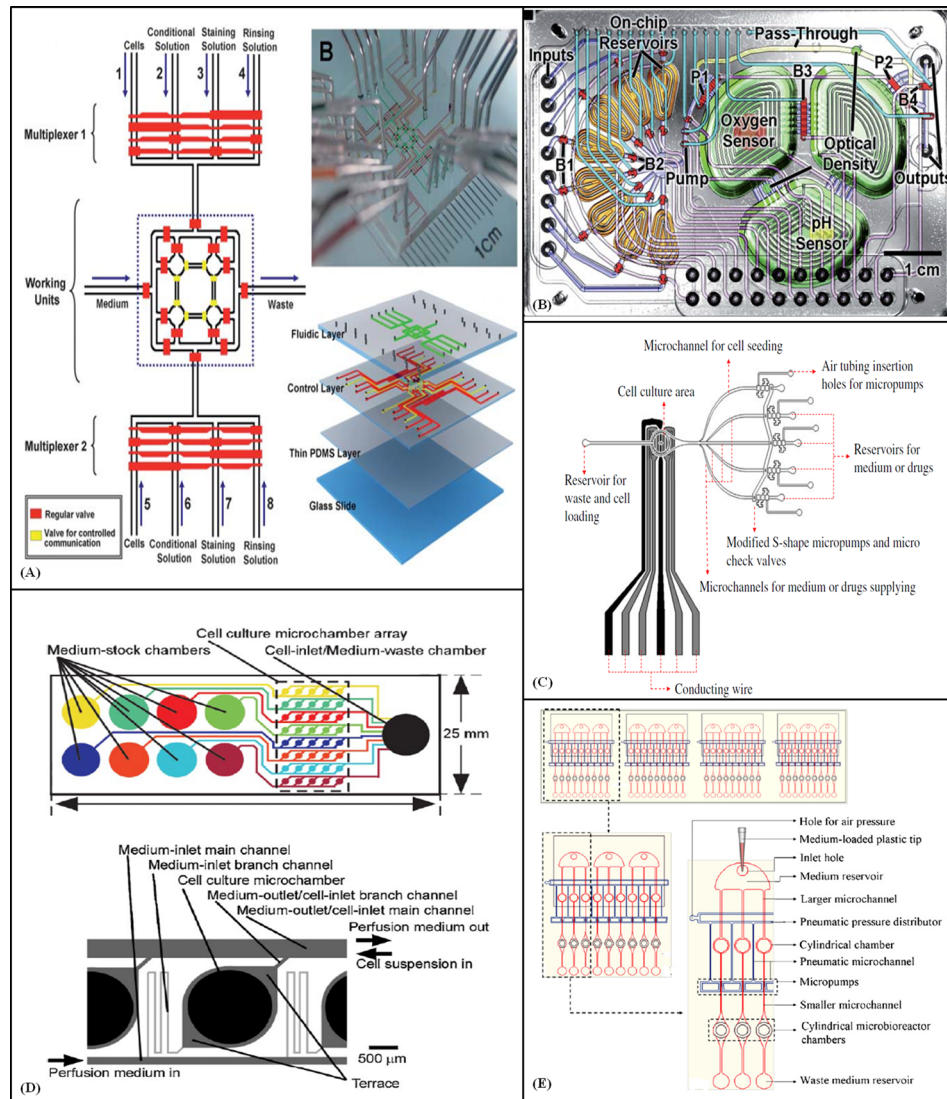


FIG. 2. Integration and multiplexing. (A) Four layer integrated microfluidic system for studying cell-microenvironmental interactions with four culture chambers. Reproduced by permission from Liu *et al.*, *Lab Chip* **10**, 1717–1724 (2010). Copyright 2010 by The Royal Society of Chemistry. (B) An automated and continuous cell culture device. Reproduced by permission from Lee *et al.*, *Lab Chip* **11**, 1730–1739 (2011). Copyright 2011 by The Royal Society of Chemistry. (C) Illustration of a platform comprising modules for cell culture and temperature control. Reprinted with permission from Hsieh *et al.*, *Biomed. Microdevices* **11**(4), 903–913 (2009). Copyright 2009 Springer Science+Business Media (Figure 1(a)). (D) Microchamber array and microchannel networks of the perfusion culture chip. Reprinted with permission from Sugiura *et al.*, *Biotechnol. Bioeng.* **100**, 1156–1165 (2008). Copyright 2008 Wiley Periodicals, Inc., John Wiley and Sons. (E) Top view layout of the microfluidic cell culture chip, the close-up view of each section, and each cell culture unit. Reprinted with permission from Wu *et al.*, *Sens. Actuators, B* **155**(1), 397–407 (2010). Copyright 2010 Elsevier.

microfluidics for adherent cell studies. To construct systems that were well suited for both cell growth and droplet actuation, they covered the device with Teflon-AF and then coated isolated parts with ECM proteins to form adhesion pads. To replenish growth media, a large droplet of fresh solution was moved across the pad to collect the old media and leave new media behind, driven by the difference in surface hydrophilicities. Three of these “passive dispensing” exchanges were sufficient to completely replace the growth media. Different types of cells (CHO-K1, HeLa, and NIH-3T3) were cultured in droplets for several days with proliferation rates similar to macro-scale cultures. In order to subculture in the second half of the exponential growth phase, cells were detached by simply replacing the media with trypsin, and then a new

droplet of media was used to collect some of the cells and move them to a secondary adhesion pad. Approximately, 2% to 3% of the cells were delivered to the new adhesion site per droplet. The same research group used digital microfluidic platforms for reagent dispensing, cell culture, and analysis.^{63–65}

c. Drug screening. Pre-clinical drug screening using multiplexed microfluidic chips allows efficient analysis of small volumes of drugs and cells to develop low cost and higher throughput assays. A microfluidic hepatocyte culture system for multiplexed *in vitro* drug testing was developed by Toh *et al.*⁶⁶ The device contained eight parallel channels with dimensions of 1 cm length, 600 μm width, and 100 μm height. An array of elliptical micropillars (30 μm \times 50 μm) divided each channel into a 200 μm wide central cell-culture compartment and two side perfusion zones. The cell suspension was introduced into the central compartments through a single inlet. The side perfusion zones were independently addressed by a linear concentration gradient generator (CGG). The culture medium was injected at a flow rate of 90 $\mu\text{l/h}$. Hepatocytes were successfully cultured within these microenvironments, and the hepatotoxicity of five model drugs was assessed.

A microfluidic cell culture platform with integrated microheaters, temperature sensor and micropumps for real-time examination and assessment of cellular functions (Fig. 2(C)) was described by Hsieh *et al.*⁶⁷ The cell culture module (CCM) consisted of five reservoirs for medium or drugs, which were delivered to a thin micro-culture chamber (180 μm depth, designed for high-resolution cellular and sub-cellular imaging) via microchannels (500 μm wide initially and 5000 μm wide at the culture area) controlled by S-shape pneumatic micropumps and check valves. A temperature-control module maintained the cell culture environment at 37 °C. The influence of shear stress was minimised by the low flow rate and a series of ring-shape pillars that encompassed the cell culture area. An oral cancer cell suspension was pumped into the micro-culture area and the medium was introduced at a flow rate of 9 $\mu\text{l/h}$. The mitotic activity and the interaction between cells and anti-cancer drugs were observed. For drug cytotoxicity assay, Sugiura *et al.*⁴⁶ presented a pressure-driven perfusion cell culture system with an 8 \times 5 array of independent microchambers, each with 1430 μm diameter and 180 μm depth (Fig. 2(D)). Terrace structures (65 μm depth) were created around chambers to assist the removal of air bubbles during cell loading and to distribute the medium flow uniformly. With a 5 kPa medium-stock chamber pressure, a shear stress of 10^{-5} Pa was induced on cells. The device was successfully utilised for a parallel cytotoxicity assay of seven anticancer drugs on HeLa cells from human cervical carcinoma, involving 3 days of continuous perfusion with seven different drug-containing media and one negative control media.

A microfluidic cell culture array with an integrated combinatorial mixer for cell-based assays was reported by Liu and Tai.⁴⁷ The device was composed of a Parylene C chip and a PDMS chip, with a porous polyethylene terephthalate (PET) membrane (0.4 or 1.0 μm pores) sandwiched in between the two chips. The bottom face of the Parylene chip contained the combinatorial mixer channels (14 μm height) and the top face contained the chambers, overpasses and outlet channels (25 μm height). Compounds from the three inlets were delivered into the eight chambers with different combinations, at concentrations determined by the fluidic resistance of the channels. The PDMS chip had 100 μm height channels creating a cell loading inlet and eight culture chambers (600 μm diameter) aligned to the chambers of the Parylene chip. The diffusion of solutions through the PET membrane within the chambers enabled efficient collection of cells without attachment factors, and ensured low shear stress on the cells during assays. B35 rat neuroblastoma cells were cultured and the ability of three compounds (at a flow rate of 5 $\mu\text{l/min}$) to alleviate hydrogen peroxide cytotoxicity was evaluated. They also tested the cytotoxicity of three chemotherapeutic agents (at a flow rate of 10 $\mu\text{l/min}$) on human breast cancer cells (MDA-MB-231).

A microfluidic 3D platform for uniform and stable cell culture environments has been fabricated by Wu *et al.*⁴⁸ The key design feature of this six-layer laminate structure was the delivery of culture medium from reservoirs to the microbioreactors by 30 S-shape pneumatic micropumps (coupled to a single pneumatic tank), integrated with an efficient cell/Agarose (scaffold)

loading system. Each reservoir supplied three bioreactors, allowing replication of experimental conditions. The 3D cell culture area of each bioreactor was a cylindrical chamber with diameter of $900\ \mu\text{m}$ and height of $220\ \mu\text{m}$. By applying a negative pressure, the cell/agarose suspension was loaded into the bioreactors through microchannels. The pneumatic micropumps then continuously supplied the culture media at a flow rate as low as $8.5\ \mu\text{l/h}$, providing an adequate nutrient supply whilst limiting shear stress. In a preliminary demonstration, the viability of oral cancer cells over a 48 h culture period remained as high as 95%–98%. For chemosensitivity assays, Wu *et al.*⁴⁹ subsequently reported a high-throughput microfluidic 3D cell culture system containing 36 microbioreactors. The device contained four sections, each with nine microbioreactors (Fig. 2(E)). As above, each medium reservoir supplied three microbioreactors, which in this case enabled the simultaneous evaluation of 12 different culture environments in triplicate. The medium was delivered to the cylindrical microbioreactor chamber (D: 1.5 mm, H: 1 mm) by a pneumatically driven membrane-based micropump at a uniform flow rate between 1.2 and $3.9\ \mu\text{l/h}$. The chamber had a shallow cylindrical cavity (D: 1 mm, H: $250\ \mu\text{m}$) to accommodate the cells/scaffold for 3D cell culture. The pneumatic micropump consisted of two pneumatic microchannels around the medium microchannel. The thickness of the PDMS membrane between these two microchannels at the upstream and downstream sides varied between $40\ \mu\text{m}$ and $60\ \mu\text{m}$. By deformation of PDMS membrane with pneumatic pressure, a peristaltic effect was produced to deliver the medium by means of this simple design. The cell/hydrogel suspension was manually loaded by assembling the lower PDMS layer of the chip with an alternative top layer to create a flat surface with the cavities exposed. The suspension was then spread across the surface, and the lower layer was removed and connected with the upper layers of the chip. A chemosensitivity assay of an anti-cancer drug with human colorectal adenocarcinoma cell culture (36 h) was demonstrated.

The same research group described a similar device with 48 individual microbioreactors for 3D cell culture based assays.⁵¹ In that study, the culture medium was continuously delivered by a pneumatically driven, membrane-based C-shaped micropump with a flow rate of $1.5\ \mu\text{l/h}$ to cylindrical microbioreactor chambers (D: 2.2 mm, H: $400\ \mu\text{m}$). Primary articular chondrocytes encapsulated in agarose gel were loaded into the cylindrical cavities of the microsystem and the effects of extracellular pH on the metabolic and biosynthetic activities of the chondrocytes were assessed. This group recently proposed a high throughput and user-friendly three-dimensional microfluidic cell culture system containing 30 microbioreactors (3 mm diameter and 2.5 mm height). By using a heater chip, stable thermal conditions for cell cultivation was provided and non-mechanical pneumatically driven multiplex medium perfusion mechanism (1.6 to $40.7\ \mu\text{l/h}$) was utilised.⁶⁸

For anti-cancer drug screening, Chen *et al.*⁵² developed a microfluidic array for 3D cell culture. The device consisted of 32 flow units on a standard 96 well plate where each unit had 3 wells (flow inlet, cell culture chamber, and flow outlet). Human mammary epithelial cell line MCF-10A was used to examine cell growth and differentiation to form distinct basal and apical polarity over 9 days. Cells were cultured with gravity driven perfusion by adding $300\ \mu\text{l}$ to the flow inlet well and $30\ \mu\text{l}$ to the flow outlet well with a fluidic resistance that allowed $80\ \mu\text{l}$ fluid flow every 24 h. Cells and Matrigel mixture was placed into the open access culture chamber. The measured flow rate which was not affected by the presence of Matrigel was $5\ \mu\text{l/h}$ for the first 24 h, then decreased to $3\ \mu\text{l/h}$ for the second 24 h, and balanced within 3 days. For long term culture and continuous flow, medium was refilled every 2 days. Perfusion channel was a microfabricated perfusion barrier ($75 \times 4 \times 4\ \mu\text{m}$ (L \times W \times H)) around the culture area (2 mm diameter) that acted as a barrier for gel while allowing diffusion of medium. MCF-10A mammary epithelial cells cultured in Matrigel demonstrated acinus morphology over 9 days. The application of the microfluidic array for *in vitro* anti-cancer drug screening was also investigated. A microfluidic device containing array of microwells was developed for spheroids of HT-29 human carcinoma cell culture and a cytostatic drug investigation.⁶⁹ The device consisted of three microchannels with 1 mm width and $50\ \mu\text{m}$ depth and 15 microwells with $200\ \mu\text{m}$ diameter and $150\ \mu\text{m}$ depth. Media was injected to the system for 30 min every day at $4.5\ \mu\text{l/min}$. Results showed that cells response to different concentrations of drug was different and for more frequent drug dosing spheroid diameter decreased rapidly.

B. Stem cell cultivation and proliferation

Commonly used biomimetic methods and procedures to grow and maintain stem cells besides being highly expensive are mostly unrefined and do not completely mimic the *in vivo* environment of a stem cell niche. With developments in microfluidic lab-on-a-chip based methods, it is now possible to design devices that not only provide favourable controlled conditions for cell growth/differentiation but also allows analysis of stem cells at a single cell level with high reproducibility and lower costs.⁷⁰ Stem cells are classified into embryonic stem cells (ESCs) and adult stem cells. Pluripotent cells obtained from the inner cell mass of a blastocyst or an early embryo are called ESCs. Multipotent cells present in a developing embryo at various tissue sites (mesenchymal, neuronal, and hematopoietic) are adult stem cells.^{71,72} Stem cells study and investigation are crucial for injuries and diseases treatment. The potential of ESCs to differentiate into almost all cell types and unlimited number of cells has promising applications in drug screening, diseases study, and tissue engineering.²³ Conventional methods for stem cells cultivation on tissue culture plastics or feeder layers with periodic exchange of medium have restrictions to investigate the self-renewal and differentiation of stem cells and tissue engineering applications.²⁰ Growth factors, signaling molecules, and cellular microenvironments play critical roles in the regulation of self-renewal and differentiation of human ESCs (hESCs). Microfluidic devices with controlled environments integrated with pumps and valves to deliver and isolate solutions are ideal for stem cells cultivation.⁷³

1. Embryonic bodies (EBs) and colonies formation and differentiation

Formation of 3D cell masses called the embryoid bodies is the first step that ESCs undergo before differentiation. This is generally achieved by growing ESCs on a cell repellent substrate. Several factors including chemical microenvironment, cell density, and the size of the colony play a key role in proliferation and directed differentiation of ESCs. The size of the embryoid bodies or the number of cells that form the initial 3D aggregate determines the differentiation of cells into specific germ layer derivatives.⁷⁴ In typical cell culture methods, large EBs are formed leading to differentiation into a heterogeneous population of cells inside the EBs. This has led to the use of 3D microwells which enables culture of size-restricted EBs on a microfluidic device. Several studies have shown that human ESC colonies can be cultured and sustained in specifically designed 3D microwells which are bordered with a non-adhesive self-assembled monolayer (SAM).⁷⁵ This size controlled micro-environment supports the renewal and maintenance of homogenous human ESCs without differentiation for longer periods than in normal 2D cultures. Besides the use of size controlled microwells, EBs have also been formed on microfluidic channels layered with semi permeable membranes. Use of non-cell-adherent polycarbonate membrane to form homogeneously sized EBs by modifying the size of the channels has been reported by Torisawa *et al.*⁷⁶ The self-aggregated ESCs remained on the membrane in the upper channel, whereas the non-aggregated cells passed through the membrane to the lower channel. Another strategy used to grow undifferentiated ESCs is the co-culture with a feeder layer coating. Mouse ESCs were cultured with a feeder layer of mouse embryonic fibroblasts using a microfluidic device with ideal flow conditions. It was established that under optimal flow conditions it was possible to maintain the actively dividing mouse ESCs without undergoing differentiation.⁷⁷ In microfluidic devices, microtraps have been also used to form embryoid bodies. Khoury *et al.*⁷⁸ reported a microfluidic device containing thousands of microtraps to position hESC for aggregation and prolonged embryoid body culturing (Fig. 3(A)). The fluid network comprised eight main interconnected microchannels with the same flow resistance. The traps contained 7 μm gaps between the segments that could be blocked with single cells or small aggregates. This design improved gas exchange and nutrient accessibility. Furthermore, unlike microwell cultures, the size of embryoid bodies (an important factor in ESC differentiation⁷⁹) was constrained in all directions because the constant medium flow inhibited growth beyond the trap opening. The geometry promoted complete trap filling, and therefore the number of cells initiating aggregation was uniform. Inner parts of the trap showed more differentiation cues. By varying flow rates, nutrient gradients across the trap region could be controlled. These microfluidic traps increased cell viability

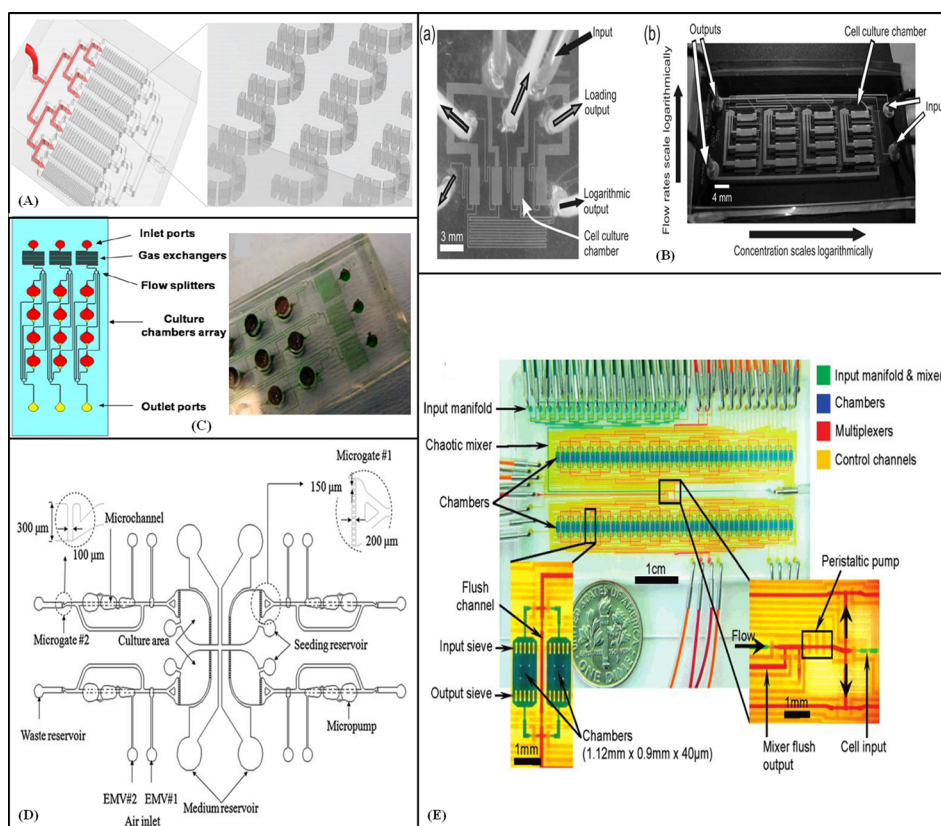


FIG. 3. Cell culture for stem cell research. (A) Illustration of a microfluidic device with microtraps for the formation of embryonic bodies. Reprinted with permission from Khoury *et al.*, *Biomed. Microdevices* **12**, 1001–1008 (2010). Copyright 2010 Springer Science+Business Media (Figure 1). (B) Photograph of (a) 1×4 and (b) 4×4 cell culture arrays with logarithmic flow rates for perfusion. Reproduced by permission from Kim *et al.*, *Lab Chip* **6**, 394–406 (2006). Copyright 2006 by The Royal Society of Chemistry. (C) Micro-bioreactor array for controlling cellular environments with four equal parts. Reprinted with permission from Cimetta *et al.*, *Methods* **47**, 81–89 (2009). Copyright 2009 Elsevier. (D) Schematic representation of the automatic microfluidic system for the culture and differentiation of stem cells with four identical modules. Reprinted with permission from Wu *et al.*, *Biomed. Microdevices* **11**, 869–881 (2009). Copyright 2009 Springer Science+Business Media (Figure 1). (E) An automated cell culture chip. Reprinted with permission from Gómez-Sjöberg *et al.*, *Anal. Chem.* **79**, 8557–8563 (2007). Copyright 2007 American Chemical Society.

and cell differentiation for more than 5 days. To provide a continuous perfusion with logarithmically scaled flow rates and studying differences in proliferation of embryonic stem cells, Kim *et al.*⁸⁰ developed two microfluidic devices for ESC cultures. The first device had four $0.32 \mu\text{l}$ cell culture chambers (Fig. 3(B-a)), each with one inlet and two output channels (a “loading” and a “logarithmic” output) that were selected with valves. The inlet for each chamber was joined to a single constant flow source. The “loading” outputs had the same fluid resistance, but the “logarithmic” outputs had resistances that increased by a factor of 6 from one chamber to the next. Murine 3T3 fibroblasts were cultured for 3 days at a total perfusion flow rate of $10 \mu\text{l/h}$, and greater cell proliferation was observed in the chamber with the fastest flow rate ($0.17 \mu\text{l/min}$). Murine embryonic stem cells were cultured at a total flow rate of $65 \mu\text{l/h}$. The majority of cells remained undifferentiated, and larger but fewer colonies were observed with faster flow rates. Shear stress in the device was 0.3 dyn/cm^2 at the fastest flow rate, which had a minimal effect on the cell cultures. They also designed a 4×4 array device (Fig. 3(B-b)) that integrated the logarithmic flow rate operation with a logarithmic concentration gradient by incorporating an on-chip diluter. To investigate the under layer material stiffness influence on cell culture, Shi *et al.*⁸¹ proposed a cell culture device with a thin film of PDMS coated on surface of different materials. MEFs, embryonic stem cells, and cerebella granule cells were tested because of their different mechanic responses. Cells were cultured in PDMS microchambers connected with microchannels for fluid flow. Experiments showed that too

soft and too hard surfaces were not appropriate for MEF cell culture while for ES cells, a harder surface increased both adhesion and EB formation and for cerebella granule cells, a softer surface improved neuron network forming. To investigate the differentiation of embryoid bodies, Kim *et al.*⁸² proposed a microfluidic device for studying the impact of soluble cues on differentiation of embryoid bodies from mouse embryonic carcinoma cell cultures. The size of the embryoid body was controlled by the initial number of cells trapped in the microwells (D: 300 μm , H: 330 μm) that depended on the cell density, flow rate, and duration time. The cell suspension was introduced at a flow rate of 0.2 ml/h by a microsyringe pump. The upstream channels had identical flow resistance and the same numbers of cells were collected in each microwell. The trapped cells formed a spherical cell body for 3 days. By chemical treatment, differentiation of the cells was achieved and observed through the *in situ* immunostaining of neuronal lineage markers.

In order to direct the stem cell differentiation on a microfluidic device, it is crucial to estimate the role of various biological factors (e.g., growth factors, glucose, oxygen, etc.).^{83,84} Controlled environments are necessary for differentiation of embryonic bodies, otherwise these cells rapidly differentiate in an uncontrolled way. Controlling the fluidic properties, such as convection, diffusion, and reaction, microfluidic devices can tune the microenvironment around the stem cells in a variety of ways that can help the cells to proliferate.⁸⁵ The cells cultured in such constrained conditions can then be differentiated into specific cells upon removal from microwells in appropriate growth conditions.⁷⁵ Mohr *et al.*⁷⁵ have demonstrated the use of 3D microwell chambers with 100–300 μm microwells that were able to control EB size of human ESCs to form cardiomyocytes. Similar studies for differentiating human ESCs and murine induced pluripotent stem cells into cells of cardiac lineage using agarose microwells have also been reported.⁸⁶ Villa-Diaz *et al.*⁸⁷ utilised a microculture system for testing single human-ESC colonies in both dynamic and static conditions for cell self-renewal and differentiation. The device had three inlet channels that converged into a cell-culture channel. The channels each had a height of 200 μm , width of 1 mm and length of 10 mm, and were bonded to a 100 mm tissue culture dish. Fluids were initially introduced into the matrigel coated microchannels by gentle aspiration at the outlet or gravitational forces in the inlet. For static culture, media was partially replaced each day, but for dynamic culture, media was delivered by a syringe pump at 0.5 ml/h per inlet. Depending on the number of inlets employed, the total flow rate in the cell-culture channel was either 1.0 or 1.5 ml/h. The resulting shear stress of up to 0.6 dyn/cm² did not affect cell adhesion and differentiation. Undifferentiated cultured hESCs were kept a normal karyotype and were capable of differentiating into ectoderm, mesoderm and endoderm. Cell proliferation was not different between dynamic and static cultures.

Shin *et al.*⁸⁸ presented an axon-isolating microfluidic device for ESC-derived neurons to study neurodegenerative diseases such as axonal regeneration. The device consisted of two channels (containing holes) and joined by microgrooves. Once middle-stage (5–7 days) embryoid bodies were localised in the main channel, the neurons were selectively cultured by changing the differentiation medium and the axons were isolated by passing through the microchannels. Cimetta *et al.*⁸⁹ designed an array of micro-bioreactors combined with a microfluidic platform for hESC cultivation studies in monolayers or 3D hydrogels (Fig. 3(C)). The platform consisted of a 4 × 3 array of cylindrical chambers (3 mm diameter), microchannels with cross section of 100 × 100 μm , three inlet ports connected to a set of four chambers with equal flow resistances and serpentine-like gas exchangers for maintaining the physiological levels of carbon dioxide and oxygen. For 2D cultivation, cells were seeded on a collagen coated surface and for 3D configuration cells were encapsulated in hydrogel. The medium was introduced by syringe pump at a flow rate of 0.3 $\mu\text{l}/\text{min}$. The low-shear conditions did not affect cell adhesion and morphology. Cell density and bioreactor configuration were both seen to influence cell differentiation.

2. Adult stem cells culture

To assess the ability of mesenchymal stem cells (MSCs) to differentiate toward hepatic cells, a simple PDMS microfluidic device with a cell culture chamber (3000 μm diameter and 100 μm deep) connected to inlet, outlet, and cell-seeding channels, was constructed by Ju

*et al.*⁹⁰ Human bone marrow MSCs were introduced into the microchamber through the seeding channel and the hepatic differentiation medium was pumped into inlet reservoirs at 0.1 $\mu\text{l}/\text{min}$ using a syringe pump. Differentiated cells expressed hepatocyte-specific markers after 4 weeks. Cells cultured within the device showed more positive signals than cells cultured on plates for comparison. Yang *et al.*⁹¹ developed a microfluidic device with nanoscale patterns for cell cultivation by means of stitching and microtransfer assembly techniques with polymer thin film technology. Human MSCs (hMSCs) were cultured on a nanopatterned area and the influence of nanotopographical and flow-induced mechanical cues on cell adhesion, migration, morphology, proliferation, and differentiation were investigated. Culture medium was pumped into four microchannels (W : 500 μm , H : 53 μm , L : 2 cm) by a syringe pump with flow rates 0.02 to 0.1 ml/h, which caused calculated fluid shear stress of 0.006 to 0.03 N m^{-2} , respectively. The microchannels had nanopatterns of 350 nm in width, 700 nm in pitch, and 280 nm in depth for mimicking the nanotopography of ECM. A two layer microfluidic device (top fluid delivery layer, and bottom culture and growth layer) was fabricated and tested for culture of primary rat hippocampal neurons prepared from E18 embryonic rats by spatio-temporal solute delivery to separate parts of neurons. The culture layer included an array of axonal channels, vertically perpendicular to the fluid delivery channels with high hydraulic resistance to maintain the desired solution. They showed cell viability and growth within the device for 11 days.⁹²

3. Integration and multiplexing

Providing environments for long-term culture and differentiation of stem cells under a steady and sustainable condition has a significant impact on stem cells research and study. Integrated microfluidic devices by incorporating micropumps to provide continuous media are reliable for this approach. Wu *et al.*⁹³ presented a new microfluidic system for automated culturing and differentiating of amniotic stem cells. Their device consisted of four equivalent modules (Fig. 3(D)), with cell culture areas designed to eliminate dead volume, which can cause the production of bubbles and cell damage. Rectangular microgates with 50 μm gaps in the culture area cut the shear force of the medium flow. Pneumatic micropumps (composed of three air chambers with different volumes) sucked the medium to the waste reservoir to maintain a continuous culture system (flow rate of 1.7 $\mu\text{l}/\text{min}$). An active microvalve and a side-channel prevented the backflow into the culture area. A comparison of a reference slide and the microfluidic system showed a small difference between the doubling times of cell populations. Amniotic fluid mesenchymal stem cells were cultured and different kinds of differentiation were realised. In an earlier study, Gómez-Sjöberg *et al.*⁹⁴ built an automated microfluidic device to create customised cell culture conditions within 96 rectangular chambers (H : 35–40 μm , V : 60 nl). As depicted in Fig. 3(E), up to 16 different fluid inputs were connected to a chaotic mixer (L : 4.8 cm, W : 130 μm) and multiplexer to distribute the fluid to any chamber or group of chambers. A peristaltic pump composed of three valves in series (located at the root of the multiplexer) enabled injection of very precise doses. Another multiplexer was used to direct the waste of each chamber. Human primary MSCs were seeded in the chip (fibronectin was used for cell adhesion) and fed with fresh media every hour. Cell proliferation and differentiation on chip were similar to standard tissue culture. The maximum shear stress on the cells with a medium flow rate of 6.5 nl/s was 0.05 N/m^2 which did not affect differentiation or proliferation. It was reported that 4 days of stimulation was needed for differentiation into the osteogenic lineage and that the motility of cells was reduced during the stimulation.

Kamei *et al.*⁷³ fabricated a semi-automated, integrated microfluidic device for the quantitative culture and analysis of hESC colonies. The device consisted of four inlets and two outlet channels, six cell culture chambers (L : 3000 μm , W : 500 μm , H : 100 μm ; total volume: 150 nl) and hydraulic valves and pumps for each cell culture chamber. Solutions were loaded into the cell culture chambers from inlets 1-3. Freshly dissociated hESC clusters were introduced by gravity flow via inlet "1," enabling visual inspection of every colony within the serpentine microchannel. To have uniform colonies, only $100 \pm 20 \mu\text{m}$, disc-shaped hESC clusters were chosen for seeding, and about four to six hESC colonies were placed in each cell culture

chamber. A ruler was fabricated alongside each chamber to characterise the locations of individual hESC. Media was introduced by peristaltic pump every 12 h. Parallel tests of proliferation or controlled differentiation were demonstrated.

III. CULTIVATION WITH GRADIENT GENERATOR DEVICES

Tissue cells are exposed to biochemical cues in the extracellular space. The concentrations of these biochemical signals such as growth factors, chemokines and hormones change spatially and temporally, and cellular behaviour depends on these signal gradients.^{95–97} Microfluidic technologies offer many opportunities to mimic the cell-cell and cell-ECM interactions of tissues. Gradient generation inside microfluidic devices has been accomplished by controlled diffusion between streams of laminar flow^{98–107} or a source and sink with different concentrations.^{108–122} High fluidic-resistance microchannels,^{108–110} hydrogels,^{111–116} or membranes^{119–122} have been used as barriers to create a free-convective-flow region between a source and sink. Several excellent reviews of biomolecular gradients in cell culture microsystems have been published.^{31,123} In this section, we focus on devices published in recent years, with discussion divided into the various approaches to establish the diffusion-based transfer of molecules. Applications for different methods of gradients generating have been presented in Sec. V. Gradient generating devices based on streams of laminar flow with parallel channels and stepwise concentrations have been widely used in drug screening. Migratory behaviour and responses of cells have been successfully investigated inside diffusion-based devices containing hydrogel or membranes. Also by means of microchannels as barriers and 3D hydrogels, neurite growth and guiding has been induced.

A. Gradient-generating devices based on streams of laminar flow

Gradient-generating networks based on parallel laminar flowing streams have been exploited in several microfluidic devices for cell culture. Wang *et al.*,⁹⁸ for example, designed a microchip that consisted of 5 gradient generators and 30 cell chambers ($2.5 \text{ mm} \times 1.25 \text{ mm}$) for seeding, culture, and stimulation. To improve cell positioning and seeding, arc-shaped weir structures were fabricated in each chamber. A syringe pump was connected to a common central outlet for cell injection and fluid transport. Reagents at different concentrations were loaded into the two inlets of each gradient generator at a flow rate of $20 \mu\text{l/h}$ and successive splitting, combining, and diffusive mixing steps delivered six distinct concentrations to the chambers. The same research group⁹⁹ subsequently published a similar device with a single gradient generator that fed a series of six cell culture chambers ($L: 2 \text{ mm}$, $W: 1 \text{ mm}$, $D: 30 \mu\text{m}$) containing dam and weirs structure for cell positioning and seeding. The cell suspension was introduced through the outlet at a flow rate of $0.2 \mu\text{l/s}$ and cells were perfused overnight with culture medium at $20 \mu\text{l/h}$. With these devices, the dose dependent effects of various chemical stimuli on the intracellular glutathione levels and drug sensitivity of human breast cancer cells (MCF-7) were evaluated.

Li *et al.*¹⁰⁰ presented a microfluidic device for generating multi-molecular gradients of permissive and inhibitory cues for guiding neurite outgrowth. Solutions were injected into inlets with a syringe pump with a flow rate of $0.2 \mu\text{l/min}$ and the molecular concentration varied linearly across the $250 \mu\text{m}$ width of each gradient channel. The generated protein gradients were adsorbed onto glass substrates coated with poly-L-lysine to shape substrate-bound gradients. Their results showed that neurites of dorsal root ganglia neurons responded toward regions of lower inhibitory chondroitin sulfate proteoglycan and higher permissive laminin concentrations. With two contrasting molecular cues presented together, neuritis responded in a different way depending on the directions of the gradients.

Wang *et al.*¹⁰¹ designed a device that created precise gradients of soluble cues for complex growth cone responses at low shear stress (Fig. 4(A)). The device consisted of a gradient generating network, a symmetric cell seeding network, and a chamber ($2 \text{ mm} \times 7 \text{ mm} \times 130 \mu\text{m}$) for cell culturing and chemotaxis observation. An upper layer of the chip contained pneumatic valves to control the flow in the bottom layer channels. An array of micro-wells etched into the glass coverslip protected the neurons from shear stress during assays. *Xenopus* embryonic

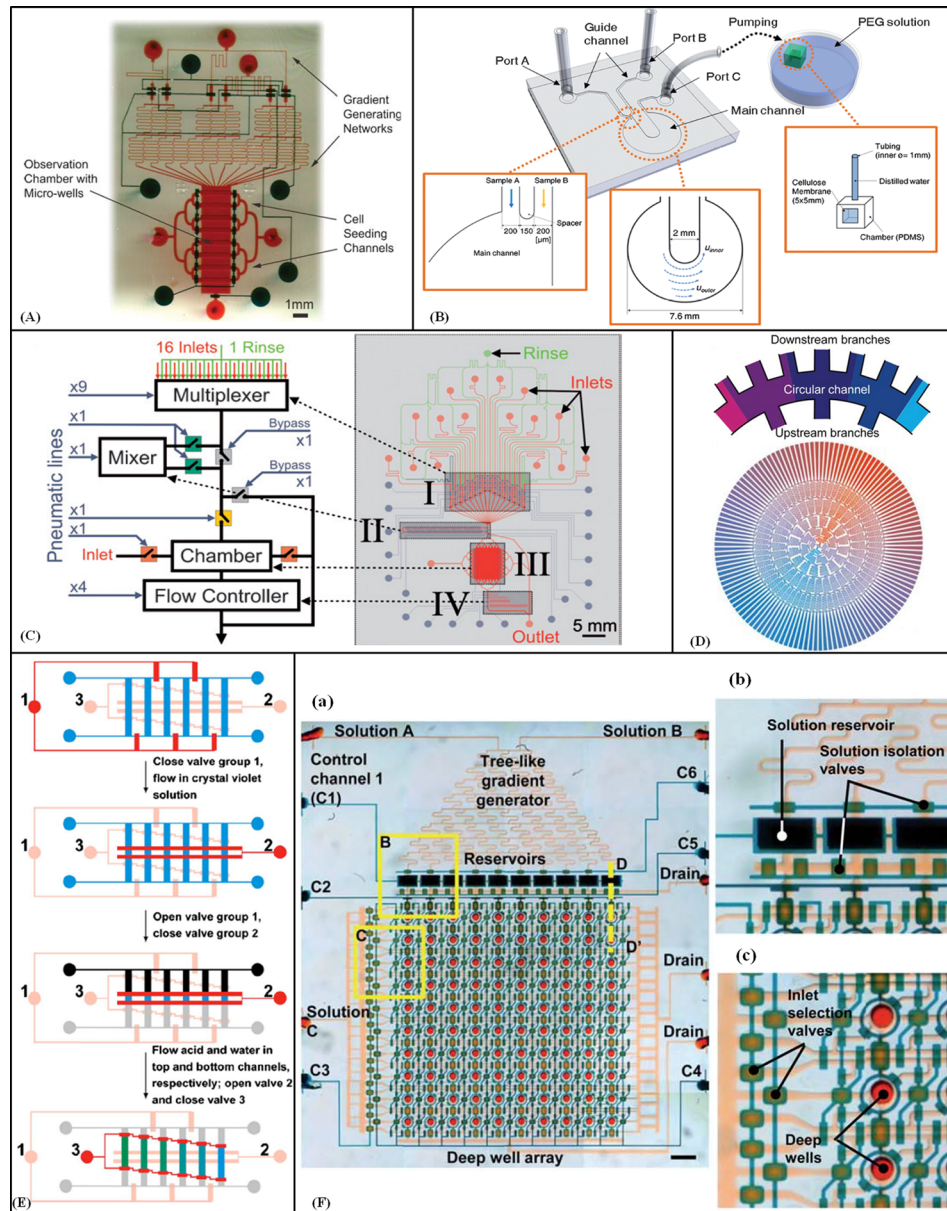


FIG. 4. Gradient-generating devices based on streams of laminar flow. (A) A device composed of two microfabricated PDMS layers containing gradient-generating network, cell seeding channels, observation chamber and control valves. Reproduced by permission from Wang *et al.*, *Lab Chip* **8**, 227–237 (2008). Copyright 2008 by The Royal Society of Chemistry. (B) Schematic of chemical and mechanical gradients generator device with a circular main channel. Reproduced by permission from Park *et al.*, *Lab Chip* **9**, 2194–2202 (2009). Copyright 2009 by The Royal Society of Chemistry. (C) Multipurpose and computer-controlled microfluidic perfusion device. Reproduced by permission from Cooksey *et al.*, *Lab Chip* **9**, 417–426 (2009). Copyright 2009 by The Royal Society of Chemistry. (D) Fluid distribution with the branch channels and the circular channels of the 2-inlet radial gradient generator. Reproduced by permission from Yang *et al.*, *Lab Chip* **11**, 3305–3312 (2011). Copyright 2011 by the Royal Society of Chemistry. (E) Operation of the microchip to generate stepwise gradient. Valve channels groups are shown (red = closed and pink = open). The fluidic channels are in the shape of a ladder (blue, grey, and black colours stand for different solutions). Reprinted with permission from Dai *et al.*, *Biomicrofluidics* **4**, 1–14 (2010). Copyright 2010 American Institute of Physics. (F) (a) 2D microfluidic combinatorial dilution device with a tree-like gradient generator (TLGG) and a microfluidic active injection system that mixes two input solutions and pre-filled solutions in wells to fill array of deep wells with different relative concentrations. (b) and (c) Enlarged view of reservoirs and deep wells. Reproduced by permission from Jang *et al.*, *Lab Chip* **11**, 3277–3286 (2011). Copyright 2011 by The Royal Society of Chemistry.

spinal neurons were seeded in wells by loading through cell inlet ports by a micropipette tip at a flow rate of $1 \mu\text{l}/\text{min}$. Utilising different valve configurations, linear or N-shaped gradients were produced by injecting low-concentration solutions to the first and third inlets and a high-concentration solution to the second inlet. A surface-bound laminin gradient (injected at flow rate of $680 \text{ nl}/\text{min}$) was found to change the polarity of growth cone responses to brain-derived neurotrophic factor ($56.7 \text{ nl}/\text{min}$) depending on concentration. The shear stress on cells without wells was $0.072 \text{ dyne}/\text{cm}^2$, while with wells it was reduced about 16-fold.

Park *et al.*¹⁰² built a microfluidic platform to generate stable concentration gradients of extracellular signalling molecules for stem cell research. Using an osmotic pump ($0.15 \mu\text{l}/\text{h}$), solutions with different concentrations were introduced from two inlet reservoirs into a channel ($W: 4 \text{ mm}$, $L: 10 \text{ mm}$, $H: 250 \mu\text{m}$), where diffusion at the solution interface created a concentration gradient. Neural progenitors derived from human embryonic stem cells were cultured in the microfluidic chamber for 8 days under continuous cytokine gradients. Cells proliferated and differentiated in a controlled manner and the cell properties clearly reflected the differing concentrations of extracellular signalling molecules.

This research group also exploited the diffusion between osmosis-driven laminar flowing solutions to combine chemical concentration and mechanical shear-stress gradients for cell culture studies.¹⁰³ As shown in Fig. 4(B), the device consisted of two inlet ports, one outlet port and a large circular channel with a 7.6 mm outer diameter and 2 mm inner diameter ($H: 100 \mu\text{m}$). The two solutions were guided into the circular channel ($0.28 \mu\text{l}/\text{min}$) where the velocity (and shear stress) in the outer region decreases. Stable gradients were created within 30 min. The shear stress within the channel was estimated to range from 0.0004 to 0.0016 Pa (at 90°). The system was tested by introducing L929 mouse fibroblast into the fibronectin-coated chip and observing their alignment, mobility, attachment, and proliferation. The alignment and migration of L929 cells depended on changes in the interstitial level of shear and their proliferation was dependent on the nutrient gradient.

Cooksey *et al.*¹⁰⁴ reported a multipurpose, computer-controlled microfluidic perfusion device with combinatorial options for cell culture conditions (Fig. 4(C)). The three-layer PDMS device contained a multiplexer for merging multiple fluid inputs from 16 inlets and one rinse channel into a single microchannel, an on/off chaotic micromixer to convectively homogenise the mixture, a bypass channel to switch the flow to the waste output, a central chamber ($5 \times 7 \text{ mm}$) containing three exits, and a microfluidic resistor to control fluid flow rates. Using combinations of dyes, a wide range of complex, dynamic gradients within the central were achieved by combining inlets, controlling mixing and regulating flow rate. When all inlets were opened into the chamber the flow rate was $44 \mu\text{l}/\text{min}$ and by closing all of the resistor valves and directing flow through the resistor channels, the flow rate was decreased to $4 \mu\text{l}/\text{min}$ which permitted more time for diffusion between streams.

Sip *et al.*¹⁰⁵ designed a cell culture microfluidic platform for generation of stable and dynamic gradients of diffusible molecules with low shear forces ($6 \times 10^{-3} \text{ dyn}/\text{cm}^2$) by stacked laminar flows. A reversible bonding with a vacuum sealing was applied so cells were cultured in a rectangular open chamber ($300 \mu\text{m}$ deep and 4 mm^2 in area). Two stacked flows in the cell culture chamber acted as a source and sink. A concentration gradient was shaped by diffusion between the laminar streams that created a stable gradient at the surface over 24 h with equilibrium time of less than 5 min. By changing the applied driving pressure, the gradients were dynamically tunable. Breast cancer cells were cultured in this device to show the negligible effect of shear flow on migration of cells.

Jedrych *et al.*¹⁰⁶ developed a microfluidic system for cytotoxicity tests. The device consisted of a 5×5 array of microchambers with a diameter of 1 mm and depth of $30 \mu\text{m}$ fabricated in a glass plate connected to series of PDMS concentration gradient generator microchannels ($W: 100 \mu\text{m}$, $H: 50 \mu\text{m}$) with two inlets and five outlets. The culturing of cells inside microchambers minimised hydrodynamic stress caused by the medium flow over the cell culture area. The medium was changed every day at a rate of $1.2 \mu\text{l}/\text{min}$ for 50 min. Human lung carcinoma cell line (A549) and human colon adenocarcinoma cells (HT-29) viability, adhesion, and proliferation were tested under different gradients of an anticancer drug (5-fluorouracil). The

inhibitory effect was dose and time dependent, similar to tests in macrosystems, although in the macroscale, the cells were more sensitive.

Yang *et al.*¹⁰⁷ designed and fabricated a radial microchannel network to generate a combinatorial, quantitative, and predictable concentration gradient by means of splitting and mixing fluids with different concentrations through six concentric circular channels ($W: 150\ \mu\text{m}$, $H: 40\ \mu\text{m}$) and parallel serpentine branch channels ($W: 80\ \mu\text{m}$, $H: 40\ \mu\text{m}$) (Fig. 4(D)). The number of branch channels doubled in each next level. The inlets were at the first level, and a wedge-shaped chamber array for cell culture ($L: 7\ \text{mm}$, $W: 100\ \mu\text{m}$ on the narrow side, $360\ \mu\text{m}$ on the wider side, $H: 40\ \mu\text{m}$) was located in the last level. Half of the source solution of the circular channel directly entered the opposite branch channel at the same concentration, while the other half of the solution flowed into the two next branches. This splitting and diffusive mixing between laminarly co-flowing streams in long branch channels was repeated to generate homogeneous solutions of different concentrations, which were introduced into the next channels to repeat the same procedure to produce a large number of different concentrations in the wedge-shaped chambers. A flow rate of $2\ \mu\text{l}/\text{min}$ at each inlet was used to guarantee the thorough diffusive mixing, which generated shear force of $0.31\ \text{dyn}/\text{cm}^2$ (acceptable for HeLa cells). In this design, the gradient could be established within 30 s with a network containing 128 cell chambers.

1. Discrete mixtures of different concentrations by dilution

A microfluidic device for the generation of stepwise concentration gradients of drugs for real-time cell apoptosis studies was developed by Dai *et al.*¹²⁴ The device had two PDMS layers (Fig. 4(E)): the bottom layer contained a “ladder” shape channel network and the top layer had three groups of microvalves to control the fluid flow. Initially, valve group 1 was closed, to force the cells to flow into the rung channels. Closing valve group 2 then enclosed the cells in central zone, whilst culture medium and drug-containing culture medium were introduced into the now separate side channels. Closing valve 3 and opening valve 2 allowed mixing of solutions with different volume ratios from the two side chambers, thus, generating a stepwise drug concentration gradient across the ladder rung chambers (each $300 \times 500\ \mu\text{m}$). With this device, apoptosis of HeLa cells under the influence of an anticancer drug at a range of concentrations was investigated.

Jang *et al.*¹²⁵ fabricated a device that included a three-like gradient generator and a microfluidic active injection system, to generate 100 discrete mixtures at different concentrations (Fig. 4(F)). Ten rectangular reservoirs ($800 \times 400 \times 300\ \mu\text{m}$, 96 nl per reservoir) were filled with graded mixtures of the two three-like gradient generator input solutions. Reservoirs solutions were injected into columns of deep wells ($D: 300\ \mu\text{m}$, $H: 300\ \mu\text{m}$ and 21.2 nl per well) pre-filled with a third solution, where flow convection and diffusion mixed the solutions. A reduced concentration solution was then introduced to the next chamber. Control channels and valves were applied to guide the fluid. In this system, a graded sequence of concentrations was produced in seconds with one injection cycle, and the concentrations could be adjusted by changing the flow rate and the number of injection cycles. Moreover, a mixture of cells and pre-filled solution could be combined in the deep wells, where cells were not under a high flow shear and during device operation the cells could be exposed to intermediate concentrations.

B. Gradient-generating devices based on diffusion from a concentrated source

1. Microchannels as barriers

Species can diffuse through interconnected microchannels that act as barriers for convective flow.^{108–110} Cimetta *et al.* developed a microfluidic device to generate stable concentration gradients for long term culture of adhering cells exposed to low shear stress.¹⁰⁸ The device consisted of three parallel channels ($W: 500\ \mu\text{m}$), with the middle channel serving as the cell culture area. An array of perpendicular microchannels ($W: 25\ \mu\text{m}$, $D: 50\ \mu\text{m}$; spaced at $50\ \mu\text{m}$) facilitated diffusion between channels to create concentration gradients. The culture channel ($V: 0.5\ \text{mm}^3$) was coated with fibronectin prior to seeding with A375 melanoma cells. Medium was

injected into the device by syringe pump at 1 $\mu\text{l}/\text{min}$ per channel, which exposed the adhering cells to a hydrodynamic shear stress of only 0.253 dyn/cm^2 .

A similar microfluidic design was adopted by Millet *et al.*¹⁰⁹ to create stable surface-bound gradients of laminin to guide *in vitro* postnatal hippocampal neuron development. By the combination of laminar flow and diffusion, different patterns and gradients of laminin and fluorescein isothiocyanate-conjugated poly-L-lysine were generated in the main channel and deposited on a glass cover slip to guide neuronal development. The results showed that when axons were exposed to both adhesive and instructional cues, elongating neurites navigated toward the increasing laminin concentration.

Bhattacharjee *et al.*¹¹⁰ developed a gradient-generator device to explore the axonal responses of mouse cortical neurons. Stable gradients of diffusible molecules were generated for at least 6 h with low shear stress inside an open chamber (H : 66 μm , W : 200 or 500 μm) enabling neurons to be cultured for at least 2 weeks. As shown in Fig. 5(A), two channels (H : 45 μm , W : 100 μm) positioned either side of the chamber acted as source and sink via arrays of microchannels (H : 2.5 μm , W : 10 μm , L : 25 μm). By frequently replenishing the gradient fluids, two constant concentration boundaries were produced in the cell culture area and a steady-state gradient formed at the surface level. The direction of flow was upward so the neurones were exposed to negligible shear stress ($<0.7 \text{ dyn}/\text{cm}^2$ at 40–150 pl/min), and thus, remained healthy for long periods of time. The majority of neurons that extended axons after being exposed to the gradients grew towards the growth factor (Netrin) source.

2. Gradients inside hydrogels

The interface between reagent solutions and the hydrogel matrices of 3D cell culture environments provides an opportunity to create diffusion-controlled concentration gradients.^{114–116} For example, Abhyankar *et al.* generated linear and nonlinear gradients of soluble factors in an agarose-filled channel connected to source and sink reservoirs,¹¹⁴ where the steady state concentration profile was defined by contents of the reservoirs and the channel geometry. Moreover, small windows in the top of the channel layer enabled dosing of the gel to create transient local gradients that did not alter the steady state concentration profiles. The source reservoir was replenished every ~ 24 h to maintain the gradient, but the timing and concentration of the fresh solution were important to avoid disturbing the system. In this manner, gradients were maintained for up to 2 days using only 34.5 μl solute. The device was demonstrated by assessing the behaviour of human neutrophils and metastatic rat mammary adenocarcinoma cells in the 3D collagen matrix in response to a gradient of epidermal growth factor over 2 days.

Alternatively, the source and sink can be maintained by continuously flowing solutions, which provides simpler handling, but with greater consumption of reagents. In one such system, designed by Haessler *et al.*¹¹⁵ for 3D chemotaxis studies, the solution channels and cell compartment (W : 400 μm ; H : 250 μm) were separated by agarose gel walls (Fig 5(B)). A cell/collagen mixture was introduced into the centre channel and different concentrations of the chemokine were injected into the side channels at 5 $\mu\text{l}/\text{min}$. After 2 h, a linear gradient was generated across the centre channel by diffusion through the agarose barrier. The buffering effect of the agarose above the chamber assisted the re-establishment of the gradient within a short period of time. Chemotaxis responses of murine dendritic cells were evaluated under gradient conditions.

Kothapalli *et al.*¹¹⁶ designed a microfluidic device to study neurite guidance under growth factor gradients, based on a T-shaped 3D gel scaffold region surrounded by three solution flow channels (Fig. 5(C)). Collagen was injected into the gel-filling channel and allowed to polymerize. Chemofactor was added to the right channel which generated a gradient across the gel (within 30 min), with the other channels acting as a sink, and neurons in the cell channel responded to the gradient. The relatively large size of the culture chamber enhanced neurite outgrowth and turning response. Using this device, the influence of known guidance cues (netrin-1, brain pulp and slit-2) on hippocampal or DRG neurite was explored. The same research group used this platform to study the chemotactic response of endothelial cells under a gradient of soluble angiogenic factors.¹¹⁷ This group recently modified their design for different cell types.¹²⁶

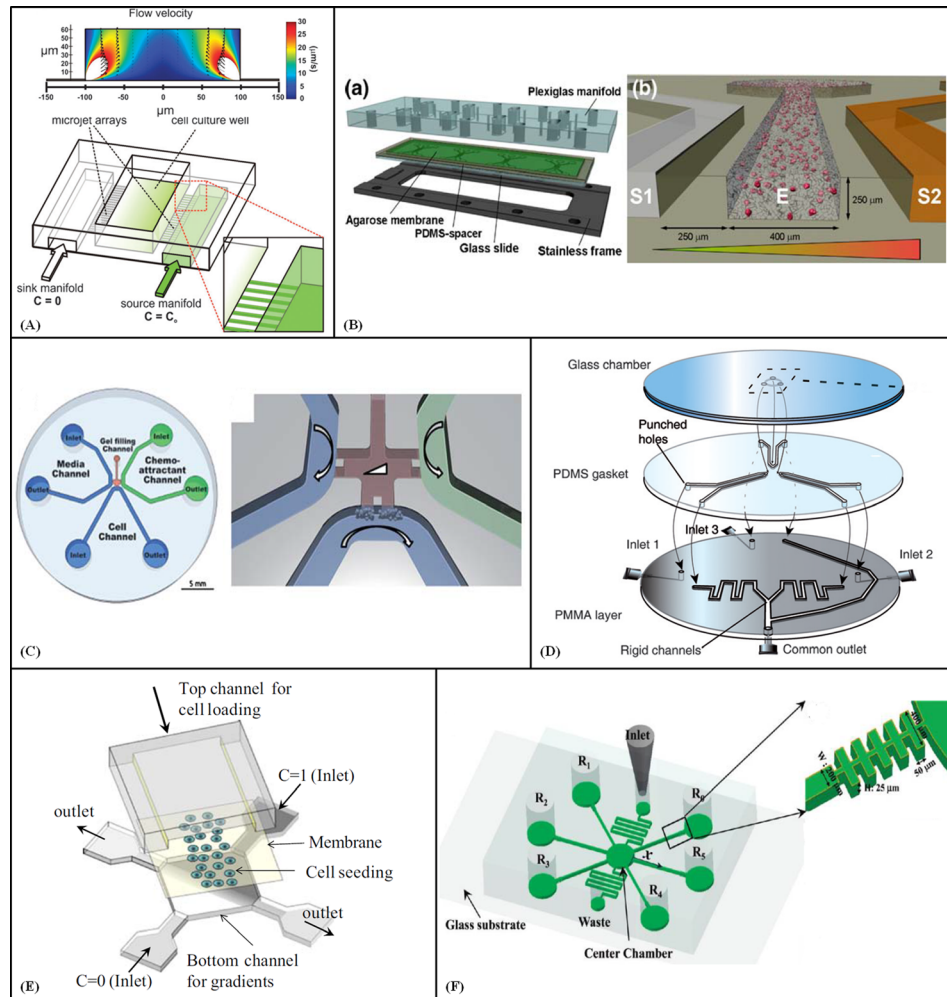


FIG. 5. Gradient-generating devices based on diffusion from a concentrated source. (A) Schematic of the device with a central open-surface reservoir (and its fluid dynamic simulation), two microchannels as sink and source and two arrays of microchannels. Reproduced by permission from Bhattacharjee *et al.*, *Integr. Biol.* **2**, 669–679 (2010). Copyright 2010 by The Royal Society of Chemistry. (B) Agarose based microfluidic device with four three-channel units. Reprinted with permission from Haessler *et al.*, *Biomed. Microdevices* **11**, 827–835 (2009). Copyright 2009 Springer Science+Business Media (Figure 1). (C) Three-channel microfluidic device developed to study neurite turning in 3D scaffolds under growth factor gradients. Reproduced by permission from Kothapalli *et al.*, *Lab Chip* **11**, 497–507 (2011). Copyright 2011 by The Royal Society of Chemistry. (D) A microfluidic device capable of generating multiple spatial chemical gradients with balanced input flow rates. Reproduced by permission from Atencia *et al.*, *Lab Chip* **9**, 2707–2714 (2009). Copyright 2009 by The Royal Society of Chemistry. (E) Schematic of the gradient generator device with a membrane separating the cell loading and gradient sections. Reprinted with permission from Kim *et al.*, *Biomed. Microdevices* **11**, 65–73 (2009). Copyright 2009 Springer Science+Business Media (Figure 1). (F) Schematic of the long-range concentration gradient generator with H-shaped channel structure. Reprinted with permission from M. Kim and T. Kim, *Anal. Chem.* **82**, 9401–9409 (2010). Copyright 2010 American Chemical Society.

Jiang *et al.*¹²⁷ developed an integrated microfluidic device for measuring the proliferation of small number of SCs (neonatal Schwann cells) in collagen gel under the mitogenic effect of platelet-derived growth factors-BB (PDGFs-BB), Fibroblast Growth Factors-base (bFGFs), and their combinations. The Microfluidic device consisted of an upstream CGG, and a downstream CCM. Different solutions were injected from the inlets at 0.1 ml/min and after mixing by diffusion in the serpentine channels and splitting, distinct compositions were generated. With one solution at zero concentration and the other one at concentration A they achieved 0, 1/7A, 2/7A, 3/7A, 4/7A, 5/7A, 6/7A, and A concentrations in the eight outlets. Cells were cultured in 0.4 ml chambers for 4 weeks at the different concentrations of growth factors. In the collagen gel,

culture cells maintained their round morphology. The results confirmed that PDGF-BB and bFGF stimulate SCs growth.

3. Diffusion with balanced input flow rates

Atencia *et al.*¹¹⁸ presented a three-layer device capable of generating multiple chemical gradients inside a microfluidic chamber, which could be held stable for long periods of time or modified dynamically. The device had a circular chamber (1.5 mm diameter; 3–20 μm thick) with three access ports that acted as sources and sinks to generate overlapping diffusive gradients (Fig. 5(D)). Solutions were introduced to the device at 0.1 ml/h by syringe pumps. As long as the flow rates through the inlet and outlet at each convection part were balanced, a diffusive gradient was generated across the chamber and with constant concentrations, constant gradients were achieved. For small molecules, about 15 min was sufficient to create stable gradients, which could be maintained indefinitely. The applicability of the device was demonstrated by studying the chemotactic response of *Pseudomonas aeruginosa* bacteria to glucose.

4. Diffusion through membranes

Membranes with appropriate pore size can also provide suitable barriers for the diffusion-controlled generation of gradients. Kim *et al.*¹¹⁹ incorporated this approach in a microfluidic device for cell culture and chemotaxis studies. The device had a fan-shaped design containing an observation chamber that was separated from the medium channels by vertical membranes with a pore size less than 100 nm. The suitability of the device for chemotaxis investigations was demonstrated with human neutrophils, which responded to the gradient of chemoattractants generated in the observation chamber by migrating to areas of higher concentration.

In another example, Kim *et al.*¹²⁰ presented a microfluidic device capable of generating steep gradients of small molecules by confronting two streams of fluids with different chemical concentrations (Fig. 5(E)). The gradient generation zone was separated from the cell culture channel (W : 500 μm , D : 80–100 μm) by a polyester membrane (0.4 μm pore diameter), to protect the cells from shear stress. The confrontation of two fluid streams created a diagonal boundary across the bottom chamber, with a steep, stable, uniform gradient. Flow rates ranging from 0.01 to 1 ml/h produced different gradients based on diffusion time. Asymmetric regions were created by controlling the flow rates and hydraulic resistances of the channels. Molecular gradients were mapped onto HeLa cells in the fibronectin-coated top channel using pH buffers and a fluorescent dye that was actively taken up by the cells.

Hydrogel plugs have also been utilised as porous membranes within a diffusion-based microfluidic gradient generator for small molecules.¹²¹ As shown in Fig. 5(F), the device consisted of a central chamber connected to six surrounding reservoirs via microchannels (W : 200 μm , H : 25 μm , L : 8 mm). Agarose plugs were integrated in H-shaped structures at the reservoir entrance of the microchannels, with diffusion through the plug creating long-range linear concentration gradients to the central chamber. Two additional channels were used to provide media and remove waste. The device was used to study the chemotaxis of bacterial cells (*E. coli*) in multi-concentration gradients of different sugars. The cells formed population bands and migrated toward higher sugar concentrations until the consumption rate by the cells equalled the diffusion rate of the carbon source. Moreover, the preferential chemotaxis of cells toward different sugars was established.

Tan *et al.*¹²² developed a simple microfluidic channel system with patterned hydrogel to generate temporally and spatially stable concentration gradients. The device was composed of parallel source and sink microchannels (W : 105 μm , H : 50 μm) connected by 24 perpendicular cross-channels (W : 310 μm , L : 317 μm , H : 50 μm) with hydrogel barriers at either end, to form static areas for cell-based assay (isolated from the main channel flows but permeable to appropriate solutes). Solutions were introduced into the microchannels at 100 $\mu\text{l}/\text{min}$ by withdrawal from the outlet. Concentration gradients were established within the first 15–20 min of perfusion. The capability of the system for cell-based studies was demonstrated by generating a

concentration gradient of a fluorescent glucose analogue over a monolayer of β -TC-6 cells, which internalised the probe.

Choi *et al.*¹²⁸ utilised enzymatically crosslinkable synthetic hydrogels to fabricate *in situ* membranes within microfluidic channels. By mixing crosslinkable solutions introduced into a microfluidic channel, *in situ* crosslinked hydrogel membranes were formed with a thickness controlled by the crosslinking reaction time and velocity. To create parallel dual hydrogel membranes, the channel (W: 3 mm and L: 13 mm) was filled with the three layers of solutions at a flow rate of 0.5 ml/min with a crosslinking reaction time of 50 s and DI water was used to wash the unreacted solutions. The microchannel separated into three parts by the parallel dual hydrogel membranes was used to generate stable chemical concentration gradients by introducing cells into center channel and reagents into the side channels at a flow rate of 1.0 ml/min. The non uniformity of hydrogel membranes thickness could alter the linearity of gradients. The device was tested with chemotaxis-dependent migration of *Salmonella typhimurium* to show the capability for chemotaxis experiments.

IV. CELL PATTERNING AND POSITIONING

A. Substrate with adhesive patterns

Utilising microfluidic devices, cell patterning has been achieved by culturing cells on a substrate with adhesive patterns. By selective deposition of molecules that affect cell adhesion on surfaces, cell growth, cultivation, and proliferation can be controlled.¹²⁹ Microfluidic patterning using microchannels and laminar flow properties can be used for patterning various cells by selectively delivering the materials for cell adhesion to the desired area of the substrate.^{130–134} Patrino *et al.*¹³⁰ produced a substrate for cell patterning by depositing thin metal films in the presence of a gaseous plasma for the surface modification of PDMS. Microdots of aluminium with 180 μm and 230 μm diameter were sputtered on PDMS with a thickness of 42 ± 4 nm. After etching the aluminium, the underlying substrate was modified. Fibroblast cells seeded on the PDMS substrates selectively adhered to these modified areas and formed multilayer structures when cultured beyond confluency. For cell-cell interactions studies and tissue engineering applications, Yamazoe *et al.*¹³¹ created patterned cell co-cultures on albumin-based substrates. At first, a cell type was attached on a cell-non-adhesive albumin substrate, and then the remaining region was changed to adherent by exposing the albumin coated substrates to UV light and polyethyleneimine for the attachment of secondary cells and creation of localised co-cultures. They demonstrated a patterned co-culture of mouse neuroblastoma Neuro-2a cells with mouse fibroblast L929 cells and a micropatterned co-culture of hemopoietic stem cells PA6 with 3T3 murine fibroblasts inside a microfluidic device. Microchannels of the microfluidic device were fabricated with the height of 50 μm and widths of 500 μm in the cell culture channel and 100 μm in the manipulation channels. The cells were cultured with the medium at a flow rate of 0.2 $\mu\text{l}/\text{min}$.

Sivagnanam *et al.*¹³² separated MCF-7 epithelial breast cancer cells from a cell solution by means of micropatterned streptavidin-coated magnetic beads patterned in the form of 50 μm -wide stripes followed by an *in situ* cell culture on the beads inside a microfluidic channel (W: 200 μm , H: 100 μm , and L: 25 mm) (Fig. 6(A)). They used a rapid magnetic-field-assisted electrostatic self-assembly procedure. Beads were coated with immunospecific cell-capture ligands and cell-adhesion-promoting proteins. Immunoluminescent analysis of the cultured cells was carried out by 5D10 biomarker expressed on the MCF-7 cell surface. Tenstad *et al.*¹³³ demonstrated the long-term cultivation of a human telomerised BM-driven mesenchymal cell line (MSCs) in a PDMS/PS microfluidic platform. They developed a patterning method for cell positioning based on the modification of a polystyrene substrate, first by selective oxygen plasma and then by patterning with Pluronic. The size of the main channel for cell cultivation was 300 μm in height, 1.5 mm in width, and 1.8 cm in length, and the perfusion channels were 22 μm in height and 50 or 100 μm in width. Adipogenic and osteogenic differentiations of MSCs were successfully demonstrated.

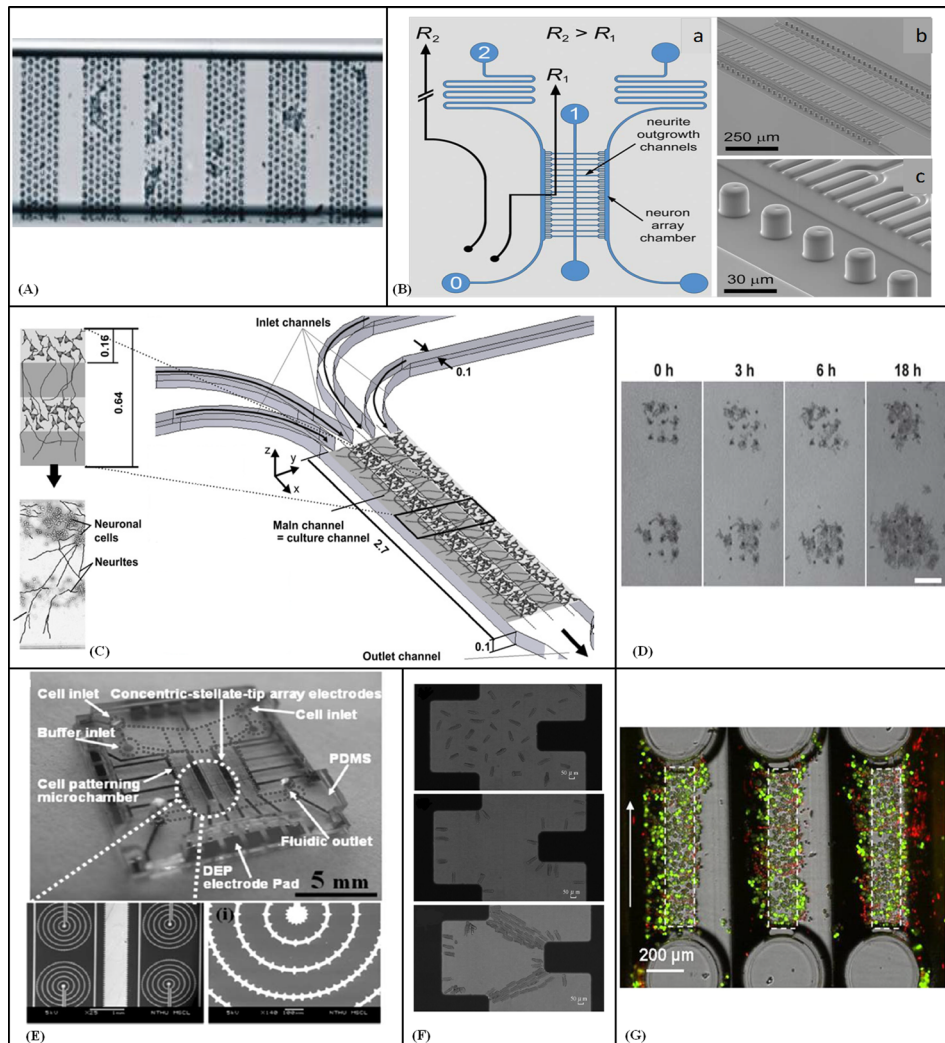


FIG. 6. (A) MCF-7 cells captured and cultured (for 4 h) on the patterned beads inside a microfluidic channel. Reprinted with permission from Sivagnanam *et al.*, *Langmuir* **26**, 6091–6096 (2010). Copyright 2010 American Chemical Society. (B) (a) Microfluidic device for single neuron arraying, with culture chambers interconnected by neurite outgrowth channels for neuron trapping. (b) and (c) SEM images of the array and Trident-shaped neuron trapping structures. Reproduced by permission from Dinh *et al.*, *Lab Chip* **13**, 1402–1412 (2013). Copyright 2013 by The Royal Society of Chemistry. (C) The layered structure of the 3D neural cell culture. The hydrogel or cell loaded hydrogel flow in through the four inlet channels, through the main channel and exit the outlet channel. Reprinted with permission from Kunze *et al.*, *Biomaterials* **32**, 2088–2098 (2011). Copyright 2011 Elsevier. (D) Cell growth and stagnation during 18 hr by loading into a 3×3 drain structure. Reproduced by permission from Zeitoun *et al.*, *Lab Chip* **10**, 1142–1147 (2010). Copyright 2010 by The Royal Society of Chemistry. (E) The cell-patterning chip, the SEM image of the electrode geometry and the close-view of the concentric ring electrodes with stellate-tips. Reproduced by permission from Ho *et al.*, *Lab Chip* **6**, 724–734 (2006). Copyright 2006 by The Royal Society of Chemistry. (F) Optical micrographs of cardiac myocytes orientation in the microfluidic device. Reprinted with permission from M. Yang and X. Zhang, *Sens. Actuators, A* **135**, 73–79 (2007). Copyright 2007 Elsevier. (G) Adherent cells after 10 min perfusion with medium. Direction of flow is indicated by arrow. The shape of the gap surface is outlined by dashed lines. Reprinted with permission from Schütte *et al.*, *Biomed. Microdevices* **13**(3), 493–501 (2011). Copyright 2011 Springer Science+Business Media (Figure 10(d)).

To produce *in vitro* cardiac tissue models Khademosseini *et al.*¹³⁴ utilised patterned hyaluronic acid (a component of the ECM found in many tissues) through microchannels (W : 100 μm and H : 60 μm). Cardiomyocytes attached to the glass substrate and the interface between the acid patterns and glass. Seeded cardiomyocytes proliferated and aligned along the pattern direction on the glass substrate. After 3 days in cultivation, contractile cardiac organoids were formed and started beating.

B. Mechanical constraints

Mechanical constraints and structures along with patterning techniques also have been used to shape the desired patterns of cells and neurite outgrowth.^{135–137} Mechanical constraints and structures like microchannels and barriers compatible with neural cells size have been used for neuronal patterning. Dinh *et al.* presented microfluidic circuits for the preparation of neuronal networks with minimal cellular inputs for the construction of compartmentalized brain models with single cell precision.¹³⁵ They used biomaterial patterning for the long term maintenance of neuronal arrangements in 3- μm -wide and 3- μm -high neurite outgrowth inlets (Fig. 6(B)). Kunze *et al.*¹³⁶ presented micropatterning of neural cell cultures in a multi-layered alginate enriched agarose scaffold, in a microfluidic device with dimensions comparable to those of neural cell layers ranging from 120 μm to 400 μm while *in vivo* developed cortical tissues consist of six cell layers (Fig. 6(C)). The microfluidic chip consisted of four inlet channels (L: 10 mm and W: 100 μm) with same pressure drop connected to cylindrical fluid reservoirs, a main channel, and one outlet channel (L: 16.6 mm and W: 400 μm) with a lower pressure drop than the inlet channels to keep the fluid in the main channel. Four parallel hydrogel layers were introduced to the main channel under laminar conditions side-by-side, with two of them containing primary cortical neurons. The hydrogel was introduced to the main channel by withdrawing from the outlet at a flow rate of 200 nl/s. By placing the microfluidic devices in petri dishes surrounded with medium, culturing of primary neural cells in the micropatterned hydrogel was feasible for 3 weeks.

Zeitoun *et al.*¹³⁷ utilised laminar convective flow for positioning particles in 2D patterns. *Saccharomyces ludwigii* yeast cells could be rapidly loaded onto vacuum-actuated holes and by a high drain density, larger systems can be produced (Fig. 6(D)). The topside fluidic layer included a fluid inlet, an outlet, and a channel to guide flow to the drain. The backside fluidic layer was a 150 μm high chamber to actuate the device drains. Cells were grown on a 3 \times 3 drain array pattern allowing the aggregated cells to be cultured.

C. DEP force

Reconstructing the complicated architectures of tissues like kidney and liver cannot be accomplished even by advanced scaffolds and therefore high resolution cell patterning is needed for this purpose.^{138–140} Another efficient way for cell positioning is DEP force which has the ability to move and spatially pattern mixtures of cells. Cells can be manipulated by DEP to form complicated structures for tissue engineering applications.¹⁴¹ Ho *et al.*¹⁴² developed a rapid liver-cell patterning microfluidic device, which operated with positive DEP to build the pattern of heterogeneous liver cells. The device imitated the lobular morphology of real liver tissue *in vivo* with proper positioning of both hepatic and endothelial cells (Fig. 6(E)). A specific snaring electrode array for the DEP manipulation of the liver cells was designed to construct the radial pearl-chain patterns. The microfluidics part of their chip was capable of manipulating, snaring, and patterning a mass of individual cells in parallel. For manipulation of cells with DEP, concentric-stellate-tip array electrodes with inhomogeneous electric-field gradients were used to guide individual cells in microfluidics to form a spatially organised pattern. Initially, the concentric-ring array electrodes supplied a global radial electric field for the configuration of cell patterning, meanwhile the concentric stellate-tips precisely snared the cells to form the desired cell pattern. Liver cells were introduced into the microfluidic chamber and then guided along the flow and dispersed at random. When the cells reached the cell patterning zone above the concentric-stellate-tip array electrodes, they were manipulated by the field-induced positive DEP from an adequate AC potential and the hydrodynamic force of suitable input flow rate. By applying a 5 V peak–peak DEP force at 1 MHz, a good cell viability of above 95% for 1-h continuous DEP manipulation with the gentle low-conductivity medium was achieved. In their experiments, the human umbilical vein endothelial cells (HUVECs) as second type of cells could only be attracted to the available local electric field maxima since the first type of cells, human liver cell line (HepG2) had occupied the area of local electric-field

maximum to form the lobule-mimetic radial pattern and reformed the electric field. As a result, the HUVECs could shape the radial pearl-chain array, to mimic the form and the role of sinusoid-like vascular endothelial lining cells in the real hepatic lobule.

Park *et al.*¹⁴³ described the use of a non-uniform electric field generated by electrodes fabricated on a printed circuit board (PCB), implementing DEP on a microfluidic channel. The microchannel was composed of a microscope coverslip and a patterned PDMS slab placed on the PCB. The disposable thin glass coverslip made the PCB reusable by isolating it from likely contamination. The manipulation of polystyrene beads and HeLa cells was achieved with negative and positive dielectrophoresis, respectively. A drop of DI water was placed on top of the electrodes to maintain indirect contact between the PDMS/coverslip assembly and the electrodes. By applying a potential with the same magnitude but opposite polarities to the adjacent PCB electrodes (76 V peak-to-peak at a frequency of 1 MHz), a non-uniform electric field was generated. Maximum and minimum squares of the electric field intensity were seen between and directly above the electrodes, respectively. Under a non-uniform electric field, HeLa cells experienced a positive DEP and moved to the high electric field regions between the adjacent electrodes. In contrast, a negative DEP placed the polystyrene beads above the electrodes. The DEP force was affected by applied voltages and the thickness of the coverslip and the width/spacing of the electrodes. By decreasing the thickness of the coverslip and the electrode spacing while keeping the magnitude of DEP force unchanged the resolution of patterning could be improved. They used commercially available 100 μm thick coverslip with 152 μm and 229 μm width/spacing interdigitated electrodes. Fibronectin coating of glass coverslip improved the attachment of the cells after turning off the DEP signals.

In cardiac muscle constructs, cell orientation plays an important role because the *in vivo* cardiac tissue is anisotropic, and according to direction of measurement, the properties of cardiac muscle are changed. Yang and Zhang¹⁴⁴ reported a cardiac tissue-like structure by means of dielectrophoresis and electro-orientation inside a microfluidic chip (Fig. 6(F)). They showed that along the electric field direction controlled by the microelectrodes, cardiac myocytes could be trapped and oriented. FEM modelling showed that by increasing the chamber height, the orientation torque, and DEP force were reduced. Utilising higher potentials or decreasing the space of microelectrodes can compensate this effect. After introducing cardiac myocytes with culture media to the flow chamber, the cells were randomly distributed on the surface between the microelectrodes with the AC power off. By applying a sinusoidal waveform, the cardiac myocytes were attracted to the edges of the microelectrodes parallel to the electric field (i.e., perpendicular to the edges of the microelectrodes). The high electric field region occurred around the corner of the electrodes, and according to electric potential distribution along the x - z plane, the most efficient dielectrophoretic traps were generated at 100 μm along the z -direction from the electrode surface.

For 3D co-culture of hepatocytes and endothelial cells, Schütte *et al.*¹⁴⁵ developed a new microfluidic system (Fig. 6(G)). The device had electrodes at the outer chamber walls for the assembly of liver sinusoids by dielectrophoresis onto the assembly gaps, and micropillars for reducing flow velocity and shear forces. After introducing hepatocytes at a flow rate of 20 to 100 $\mu\text{l}/\text{min}$, the voltage was set for a field strength of about 30 kV/m at a frequency of 350 kHz. The cells that had not been assembled into the gaps were rinsed with medium at a rate of 50 $\mu\text{l}/\text{min}$. After stabilisation of hepatocyte adhesion on the gap surfaces coated with extra cellular matrix proteins, the endothelial cell suspension was injected into the chip at a rate of 20 $\mu\text{l}/\text{min}$ and then the co-culture was perfused with medium at a rate of 3 $\mu\text{l}/\text{min}$.

V. FURTHER DISCUSSION AND CONCLUDING REMARKS

Microfluidic technology continues to emerge as an invaluable tool for research in cellular biology and related disciplines, with a remarkable range of innovative strategies and techniques already described in the open literature. The placement and localisation of cells for culturing, manipulation, and interrogation has been achieved in microfluidic devices with a degree of fluid control and automation not attainable through traditional macroscale techniques. In the most

simple microfluidic platforms, cells, nutrients, reagents, and even extra cellular matrix materials like collagen for adherent cell growth have been delivered to cell culture chambers by syringe pumps, micropipettes, or suction pumps, but as discussed in the proceeding sections, many more complicated functions involving micropumps, valves, channels, reservoirs, reactors, mixers, gates, and filters are now being introduced. Improvements in automation have been spurred by advances in micro electromechanical system technology, particularly the wider application of pneumatic pumps and valves. These simple components do not impact upon live cells, have fast response times, and are readily integrated by fabrication within PDMS membranes. Microfluidic platforms for static cell culture approaches with frequent media changing by micropipette benefit from ease of fabrication while suffer from the high risk of contamination and system perturbation. In integrated cell culture, devices with pumps, valves, and mixers continuous-perfusion are provided in a sustainable microenvironment. However, in long-term cultivation of cells, keeping the devices with peripheral tubes and compressed air supply for pneumatic pumps and valves in closed sterile autoclaves makes the experimental setup more complicated.

A crucial issue in handling cells exposed to fluidic forces is shear stress. Whilst in some cases some degree of stress has been found to induce growth and differentiation,¹⁴⁶ direct exposure to the flow rates generally required to supply sufficient nutrients is undesirable due to the damaging effect on the cells. Consequently, a wide range of approaches have been employed to protect cells from shear stress, including low flow rates,^{43,48,102} changes in channel depth,⁴² or geometry;^{103,110} incorporation of microwells,¹⁰¹ microchannels,^{108,109} grooves,⁴¹ micropillars,^{66,67} or membranes^{40,47,120,121} in or around the cell culture zone.

2D cell culture systems are appropriate in order to control large number of cells and real-time observation and analysis with fluorescence detection methods. Compared to 3D cell culture environments, 2D culture conditions are less able to mimic the real cellular surroundings inside body except for specific cells like endothelial cells.²⁶ These 2D environments cannot maintain *in vivo* cell-cell interactions, and shear stress of growth factors and even oxygen can reduce cell viability.¹ In addition, providing an accurate and efficient cell/gel loading system without human intervention and errors can improve integrated and automated cell culture systems remarkably.⁴⁸ Furthermore, constructing functional grafts for implantation can be achieved by 3D cell culture.

Microfluidic cell culture platforms are promising systems for stem cell proliferation and differentiation assays for ESCs^{73,78,80,81,87,89,102} and MSCs.^{91,93,94} These devices have been used for EBs formation and cultivation in microwells⁸² and microtraps,⁷⁸ guiding neurites outgrowth and responses in gradient generator devices,^{100,109,110,115,116} axonal isolation in microgrooves⁸⁸ or influence of mechanical cues in cell culture.^{81,91} The advantages of using microtraps to form EBs are efficient exchanging of gas/nutrients and also controlling EB size in all orientations. Since stem cells culture is a long term process, microfluidic perfusion systems can restore the vascular system to support prolonged stem cells studies. However, integrated and automated devices to provide different *in vivo* conditions for 3D stem cell cultivation and investigation are still important and ongoing works.

Table I shows a summary of cell types, culture areas, flow rates, and shear stress data for various cell cultivation and perfusion systems.

The generation of stable concentration gradients with highly regulated special and temporal control has provided the opportunity to more accurate recreate *in vivo* conditions. Flow-based gradient generators have the advantage of maintaining the steady state conditions as long as the input flows are provided, and the manipulation of gradient profiles based on flow conditions. Potential drawbacks, however, include the removal of autocrine and paracrine factors, consuming large volume of solutions and the deleterious effects of shear stress, which have been addressed in a variety of ways (see above). Diffusion-based gradient generator devices have simple designs which make them more user friendly. There is no need for peripheral equipment for input solute flow, and cells are not under the influence of shear stress. However, there is little control of concentration profiles, and the source and sink need to be replenished to maintain stable gradients. Streams of laminar flow in microchannels to generate stepwise concentrations

TABLE I. Selected data for microfluidic-based cell cultivation and perfusion systems.

Cell type	Size of culture area	Medium flow rate	Shear stress (N/m ²)	Ref.
Mouse myoblast	NA	15 nl/min	NA	61
Hepatocytes	H: 100 μ m	0.5 ml/h	NA	40
Hepatocytes	5 ml	18 ml/min	<0.033	41
Kidney Crandell feline fibroblast and immortalised mouse hippocampal	750 mm ³	24 μ l/min	NA	42
Human hepatocellular carcinoma cells and mouse embryonic fibroblasts	D: 600 μ m, H: 35 μ m	0.3 μ l/min	0.07	43
Human epithelial cells, epithelial-like breast cancer cells, and colon carcinoma cells	Depends on cell types under investigation	5 μ m/s	0.07	45
HeLa cells	D: 1430 μ m, H: 180 μ m	NA	10–5	46
Rat neuronal cells and human breast cancer cells	D: 600 μ m	5 and 10 μ l/min	NA	47
Hepatocytes	L: 1 cm, W: 200 μ m, H: 100 μ m	90 μ l/h	NA	66
Oral cancer cells	H: 180 μ m	9 μ l/h	NA	67
T-lymphocytes	H: 250 μ m	75 μ l/h	NA	59
Oral cancer cells	D: 900 μ m, H: 220 μ m	8.5 μ l/h	NA	48
Colorectal adenocarcinoma	D: 1 mm, H: 250 μ m	1.2–3.9 μ l/h	NA	49
Primary articular chondrocytes	D: 2.2 mm, H: 400 μ m	1.5 μ l/h	NA	51
Human mammary epithelial cell line	D: 2 mm	3 and 5 μ l/h	NA	52
Primary human hepatocyte	W: 100 μ m	5 μ l/h each inlet	NA	53
Hepatocarcinoma	40 μ l	0.1 and 25 μ l/min	NA	54
HT-29 human carcinoma	D: 200 μ m, H: 150 μ m	4.5 μ l/min	0.0013	69
Murine embryonic stem cells and murine 3T3 fibroblasts	0.32 μ l	10 μ l/h/65 μ l/h	0.01	80
Human bone marrow mesenchymal stem cells	D: 3000 μ m, H: 100 μ m	0.1 μ l/min	NA	90
Human embryonic stem cells	H: 200 μ m, W: 1 mm, L: 1 cm	1.5 ml/h	0.06	87
Amniotic stem cells	5 mm \times 5 mm	1.7 μ l/min	NA	93
Human mesenchymal stem cells	60 nl	6.5 nl/s	0.05	94
Human mesenchymal stem cells	W: 500 μ m, H: 53 μ m, L: 2 cm	0.02–0.1 μ l/h	0.006–0.3	91
Human embryonic stem cells	D: 3 mm	0.3 μ l/min	NA	89
Human breast cancer cells	2.5 mm \times 1.25 mm	20 μ l/h	NA	98
Human breast cancer cells	L: 2000 μ m, W: 1000 μ m, H: 30 μ m	20 μ l/h	NA	99
Neurite of dorsal root ganglia neurons	W: 250 μ m	0.2 μ l/min	NA	100
Xenopus embryonic spinal neurons	2 mm \times 7 mm \times 130 μ m	680 nl/min and 56.7 nl/min	0.0072 without wells, reduced about 16-fold with wells	101
Neural progenitors	L: 10 mm, W: 4 mm, H: 250 μ m	0.15 μ l/h	NA	102
Mouse fibroblast	W: 2.8 mm, Outer D: 7.6 mm, Inner D: 2 mm inner, H: 100 μ m	0.28 μ l/min	0.0004–0.0016	103
Neonatal Schwann cells	0.4 ml	1 ml/min	NA	127

have been widely used in drug screening. Diffusion based devices containing hydrogel or membranes facilitate the investigation of migratory behaviour and responses of cells. By means of microchannels as barriers and 3D hydrogels, neurite growth and guiding has been induced. However, localizing and packing cells in specific parts of hydrogel (not mixed with gel) may affect hydrogel stability. Table II shows a summary of gradient types of recent gradient generators.

TABLE II. Comparison of gradient generators.

Cell type	Gradient type	Method of generation	Application	Ref.
Human breast cancer cells	Stable, controlled, linear in parallel channels	Streams of laminar flow	Drug screening	98
Human breast cancer cells	Stable, controlled, linear in parallel channels	Streams of laminar flow	Drug screening	99
Neurites of dorsal root ganglia neurons	Stable, linear	Streams of laminar flow	Neurite growth and guiding	100
Xenopus embryonic spinal neurons	Stable, complex (linear and N-shape)	Streams of laminar flow	Neurite growth and guiding	101
Neural progenitors	Stable, linear	Streams of laminar flow	Differentiation of neural progenitor cells	102
Mouse fibroblast	Stable, approximately linear	Streams of laminar flow	Cell proliferation under both mechanical and chemical gradients	103
-	Stable, complex, and dynamic	Streams of laminar flow	Drug screening,	104
Breast cancer cells	Stable, dynamic controlled	Streams of laminar flow	Migratory behavior of cells	105
HeLa cells	Stable, controlled, linear, nonlinear, stepwise concentrations	Streams of laminar flow	Drug screening	107
Melanoma cells	Stable, sharp	Microchannels as barriers for diffusion)	Long term culture of adhering cells	108
Postnatal hippocampal neuron	Stable, overlapping	Microchannels as barriers for diffusion)	Neurite growth and guiding	109
Mouse cortical neurons	Short-term stable, dynamic controlled	Microchannels as barriers for diffusion)	Neurite growth and guiding	110
Human neutrophils and rat mammary adenocarcinoma	Stable, linear, exponential (with exponential channel geometry), overlapping	Gradients inside hydrogels	Migratory behavior of cells	114
Murine dendritic cells	Steady, linear	Gradients inside hydrogels	Migratory behavior of cells	115
Neurites of hippocampal or dorsal root ganglia	Short-term stable, approximately linear (steep)	Gradients inside hydrogels	Neurite growth and guiding	116
Bacterial cells (<i>P. aeruginosa</i>)	Stable, dynamic controlled, overlapping	Diffusion with balanced input flow rates	Migratory behavior of cells	118
Neutrophils	Stable, cylindrical, controlled	Diffusion through membranes	Migratory behavior of cells	119
HeLa cells	Stable, steep, symmetric, asymmetric	Diffusion through membranes	Effects of signaling molecules on cells growth	120
Bacterial cells (<i>E. coli</i>)	Steady, long range, linear	Diffusion through membranes	Migratory behavior of cells	121
Pancreatic β -cell line	Stable, linear without cells, nonlinear with cells	Diffusion through membranes	Effects of signaling molecules on cells growth	122
HeLa cells	Stable, parallel concentrations	Streams of laminar flow	Drug screening	124
Neonatal Schwann cells	Stable, parallel concentrations	Streams of laminar flow then gradients inside hydrogels	Peripheral nerve development	127

Microfluidic devices enabling of spatial arrangements of cells like a micro-tissue by dielectrophoresis,^{142,144,145} surface chemistry patterning,¹³⁴ or laminar flow of hydrogels¹³⁶ have been devised. However, new techniques to pattern tissue cells inside 3D ECMs for cultivation will improve mimicking of *in vivo* conditions.^{130–132}

The development of cell patterning, 2D and 3D cell culture systems, gradient generation, integration, and automation continue to advance, but the creation of microenvironments that are truly representative of the complex and diverse range of conditions encountered in natural living systems remains a challenging target that requires extensive further research.

ACKNOWLEDGMENTS

The authors thank Professor Stephen J. Haswell (University of Hull) for his helpful advice during the preparation of this review.

- ¹J. El-Ali, P. K. Sorger, and K. F. Jensen, “Cells on chips,” *Nature* **442**, 403–411 (2006).
- ²G. M. Whitesides, “The origins and the future of microfluidics,” *Nature* **442**, 368–373 (2006).
- ³X. Feng, W. Du, Q. Luo, and B. F. Liu, “Microfluidic chip: Next-generation platform for systems biology,” *Anal. Chim. Acta* **650**, 83–97 (2009).
- ⁴T. M. Squires and S. R. Quake, “Microfluidics: Fluid physics at the nanoliter scale,” *Rev. Mod. Phys.* **77**, 977–1026, 2005.
- ⁵C. M. Ho and Y. C. Tai, “Micro-electro-mechanical-systems (MEMS) and fluid flows,” *Annu. Rev. Fluid Mech.* **30**, 579–612 (1998).
- ⁶H. A. Stone and S. Kim, “Microfluidics: Basic issues, applications, and challenges,” *AIChE J.* **47**, 1250–1254 (2001).
- ⁷H. Andersson and A. Van Den Berg, “Microtechnologies and nanotechnologies for single-cell analysis,” *Curr. Opin. Biotechnol.* **15**, 44–49 (2004).
- ⁸P. K. Wong, T. H. Wang, J. H. Deval, and C. M. Ho, “Electrokinetics in micro devices for biotechnology applications,” *IEEE/ASME Trans. Mechatron.* **9**, 366–376 (2004).
- ⁹K. Khoshmanesh, S. Nahavandi, S. Baratchi, A. Mitchell, and K. Kalantar-zadeh, “Dielectrophoretic platforms for bio-microfluidic systems,” *Biosens. Bioelectron.* **26**, 1800–1814 (2011).
- ¹⁰K. Khoshmanesh, J. Akagi, S. Nahavandi, J. Skommer, S. Baratchi, J. M. Cooper, K. Kalantar-Zadeh, D. E. Williams, and D. Wlodkowic, “Dynamic analysis of drug-induced cytotoxicity using chip-based dielectrophoretic cell immobilization technology,” *Anal. Chem.* **83**, 2133–2144 (2011).
- ¹¹E. Kiskinis and K. Eggan, “Progress toward the clinical application of patient-specific pluripotent stem cells,” *J. Clin. Invest.* **120**, 51–59 (2010).
- ¹²C. M. Puleo, H. C. Yeh, and T. H. Wang, “Applications of MEMS technologies in tissue engineering,” *Tissue Eng.* **13**, 2839–2854 (2007).
- ¹³Y. Yang and A. J. El Haj, “Biodegradable scaffolds—Delivery systems for cell therapies,” *Expert Opin. Biol. Ther.* **6**, 485–498 (2006).
- ¹⁴H. Li, J. R. Friend, and L. Y. Yeo, “A scaffold cell seeding method driven by surface acoustic waves,” *Biomaterials* **28**, 4098–4104 (2007).
- ¹⁵M. Huang, S. Fan, W. Xing, and C. Liu, “Microfluidic cell culture system studies and computational fluid dynamics,” *Math. Comput. Modell.* **52**, 2036–2042 (2010).
- ¹⁶L. Kim, Y. C. Toh, J. Voldman, and H. Yu, “A practical guide to microfluidic perfusion culture of adherent mammalian cells,” *Lab Chip* **7**, 681–694 (2007).
- ¹⁷M. H. Wu, S. B. Huang, and G. B. Lee, “Microfluidic cell culture systems for drug research,” *Lab Chip* **10**, 939–956 (2010).
- ¹⁸E. W. K. Young and D. J. Beebe, “Fundamentals of microfluidic cell culture in controlled microenvironments,” *Chem. Soc. Rev.* **39**, 1036–1048 (2010).
- ¹⁹A. L. Paguirigan and D. J. Beebe, “From the cellular perspective: Exploring differences in the cellular baseline in macro-scale and microfluidic cultures,” *Integr. Biol.* **1**, 182–195 (2009).
- ²⁰J. A. Burdick and G. Vunjak-Novakovic, “Engineered microenvironments for controlled stem cell differentiation,” *Tissue Eng. A* **15**, 205–219 (2009).
- ²¹P. Godara, C. D. McFarland, and R. E. Nordon, “Design of bioreactors for mesenchymal stem cell tissue engineering,” *J. Chem. Technol. Biotechnol.* **83**, 408–420 (2008).
- ²²S. Kobel and M. P. Lutolf, “High-throughput methods to define complex stem cell niches,” *BioTechniques* **48**, ix–xxii (2010).
- ²³H. W. Wu, C. C. Lin, and G. B. Lee, “Stem cells in microfluidics,” *Biomicrofluidics* **5**(1), 013401 (2011).
- ²⁴Y. Huang, B. Agrawal, D. Sun, J. S. Kuo, and J. C. Williams, “Microfluidics-based devices: New tools for studying cancer and cancer stem cell migration,” *Biomicrofluidics* **5**(1), 013412 (2011).
- ²⁵G. Velve-Casquillas, M. Le Berre, M. Piel, and P. T. Tran, “Microfluidic tools for cell biological research,” *Nano Today* **5**, 28–47 (2010).
- ²⁶E. W. K. Young and C. A. Simmons, “Macro- and microscale fluid flow systems for endothelial cell biology,” *Lab Chip* **10**, 143–160 (2010).
- ²⁷I. K. Zervantonakis, C. R. Kothapalli, S. Chung, R. Sudo, and R. D. Kamm, “Microfluidic devices for studying heterotypic cell-cell interactions and tissue specimen cultures under controlled microenvironments,” *Biomicrofluidics* **5**(1), 13406 (2011).
- ²⁸D. Gao, H. Liu, Y. Jiang, and J. M. Lin, “Recent developments in microfluidic devices for *in vitro* cell culture for cell-biology research, TrAC,” *Trends Anal. Chem.* **35**, 150–164 (2012).

- ²⁹P. G. Gross, E. P. Kartalov, A. Scherer, and L. P. Weiner, "Applications of microfluidics for neuronal studies," *J. Neurol. Sci.* **252**, 135–143 (2007).
- ³⁰A. M. Taylor and N. L. Jeon, "Micro-scale and microfluidic devices for neurobiology," *Curr. Opin. Neurobiol.* **20**, 640–647 (2010).
- ³¹T. M. Keenan and A. Folch, "Biomolecular gradients in cell culture systems," *Lab Chip* **8**, 34–57 (2008).
- ³²B. G. Chung and J. Choo, "Microfluidic gradient platforms for controlling cellular behavior," *Electrophoresis* **31**, 3014–3027 (2010).
- ³³I. Meyvantsson and D. J. Beebe, "Cell culture models in microfluidic systems," *Annu. Rev. Anal. Chem.* **1**, 423–449 (2008).
- ³⁴L. G. Griffith and M. A. Swartz, "Capturing complex 3D tissue physiology *in vitro*," *Nat. Rev. Mol. Cell Biol.* **7**, 211–224 (2006).
- ³⁵D. A. Bruzewicz, A. P. McGuigan, and G. M. Whitesides, "Fabrication of a modular tissue construct in a microfluidic chip," *Lab Chip* **8**, 663–671 (2008).
- ³⁶D. Huh, G. A. Hamilton, and D. E. Ingber, "From 3D cell culture to organs-on-chips," *Trends Cell Biol.* **21**, 745–754 (2011).
- ³⁷J. Lee, M. J. Cuddihy, and N. A. Kotov, "Three-dimensional cell culture matrices: State of the art," *Tissue Eng. B* **14**, 61–86 (2008).
- ³⁸L. M. Fidalgo and S. J. Maerkl, "A software-programmable microfluidic device for automated biology," *Lab Chip* **11**, 1612–1619 (2011).
- ³⁹H. Y. Wang, N. Bao, and C. Lu, "A microfluidic cell array with individually addressable culture chambers," *Biosens. Bioelectron.* **24**, 613–617 (2008).
- ⁴⁰A. Carraro, W. M. Hsu, K. M. Kulig, W. S. Cheung, M. L. Miller, E. J. Weinberg, E. F. Swart, M. Kaazempur-Mofrad, J. T. Borenstein, J. P. Vacanti, and C. Neville, "*In vitro* analysis of a hepatic device with intrinsic microvascular-based channels," *Biomed. Microdevices* **10**, 795–805 (2008).
- ⁴¹J. Park, Y. Li, F. Berthiaume, M. Toner, M. L. Yarmush, and A. W. Tilles, "Radial flow hepatocyte bioreactor using stacked microfabricated grooved substrates," *Biotechnol. Bioeng.* **99**, 455–467 (2008).
- ⁴²G. Ciofani, A. Migliore, V. Raffa, A. Menciassi, and P. Dario, "Bicompartmental device for dynamic cell coculture: Design, realisation and preliminary results," *J. Biosci. Bioeng.* **105**, 536–544 (2008).
- ⁴³W. Liu, L. Li, X. Wang, L. Ren, J. Wang, Q. Tu, and X. Huang, "An integrated microfluidic system for studying cell-microenvironmental interactions versatily and dynamically," *Lab Chip* **10**, 1717–1724 (2010).
- ⁴⁴K. S. Lee, P. Boccazzi, A. J. Sinskey, and R. J. Ram, "Microfluidic chemostat and turbidostat with flow rate, oxygen, and temperature control for dynamic continuous culture," *Lab Chip* **11**, 1730–1739 (2011).
- ⁴⁵J. P. Frimat, M. Becker, Y. Y. Chiang, U. Marggraf, D. Janasek, J. G. Hengstler, J. Franzke, and J. West, "A microfluidic array with cellular valving for single cell co-culture," *Lab Chip* **11**, 231–237 (2011).
- ⁴⁶S. Sugiura, J. I. Edahiro, K. Kikuchi, K. Sumaru, and T. Kanamori, "Pressure-driven perfusion culture microchamber array for a parallel drug cytotoxicity assay," *Biotechnol. Bioeng.* **100**, 1156–1165 (2008).
- ⁴⁷M. C. Liu and Y. C. Tai, "A 3-D microfluidic combinatorial cell array," *Biomed. Microdevices* **13**, 191–201 (2011).
- ⁴⁸M. H. Wu, S. B. Huang, Z. Cui, and G. B. Lee, "A high throughput perfusion-based microbioreactor platform integrated with pneumatic micropumps for three-dimensional cell culture," *Biomed. Microdevices* **10**, 309–319 (2008).
- ⁴⁹M. H. Wu, Y. H. Chang, Y. T. Liu, Y. M. Chen, S. S. Wang, H. Y. Wang, C. S. Lai, and T. M. Pan, "Development of high throughput microfluidic cell culture chip for perfusion 3-dimensional cell culture-based chemosensitivity assay," *Sens. Actuators, B* **155**(1), 397–407 (2011).
- ⁵⁰Y. Gao, D. Majumdar, B. Jovanovic, C. Shaifer, P. C. Lin, A. Zijlstra, D. J. Webb, and D. Li, "A versatile valve-enabled microfluidic cell co-culture platform and demonstration of its applications to neurobiology and cancer biology," *Biomed. Microdevices* **13**(3), 539–548 (2011).
- ⁵¹S. B. Huang, M. H. Wu, S. S. Wang, and G. B. Lee, "Microfluidic cell culture chip with multiplexed medium delivery and efficient cell/scaffold loading mechanisms for high-throughput perfusion 3-dimensional cell culture-based assays," *Biomed. Microdevices* **13**, 415–430 (2011).
- ⁵²S. Y. C. Chen, P. J. Hung, and P. J. Lee, "Microfluidic array for three-dimensional perfusion culture of human mammary epithelial cells," *Biomed. Microdevices* **13**, 753–758 (2011).
- ⁵³V. N. Goral, Y. C. Hsieh, O. N. Petzold, J. S. Clark, P. K. Yuen, and R. A. Faris, "Perfusion-based microfluidic device for three-dimensional dynamic primary human hepatocyte cell culture in the absence of biological or synthetic matrices or coagulants," *Lab Chip* **10**, 3380–3386 (2010).
- ⁵⁴R. Baudoin, L. Griscom, J. M. Prot, C. Legallais, and E. Leclerc, "Behavior of HepG2/C3A cell cultures in a microfluidic bioreactor," *Biochem. Eng. J.* **53**, 172–181 (2011).
- ⁵⁵D. D. Nalayanda, C. Puleo, W. B. Fulton, L. M. Sharpe, T. H. Wang, and F. Abdullah, "An open-access microfluidic model for lung-specific functional studies at an air-liquid interface," *Biomed. Microdevices* **11**, 1081–1089 (2009).
- ⁵⁶A. Grosberg, P. W. Alford, M. L. McCain, and K. K. Parker, "Ensembles of engineered cardiac tissues for physiological and pharmacological study: Heart on a chip," *Lab Chip* **11**, 4165–4173 (2011).
- ⁵⁷A. Günther, S. Yasotharan, A. Vagaon, C. Lochovsky, S. Pinto, J. Yang, C. Lau, J. Voigtlaender-Bolz, and S. S. Bolz, "A microfluidic platform for probing small artery structure and function," *Lab Chip* **10**, 2341–2349 (2010).
- ⁵⁸C. Ronco, A. Davenport, and V. Gura, "The future of the artificial kidney: Moving towards wearable and miniaturized devices," *Nefrologia* **31**, 9–16 (2011).
- ⁵⁹P. Shah, I. Vedarethinam, D. Kwasny, L. Andresen, M. Dimaki, S. Skov, and W. E. Svendsen, "Microfluidic bioreactors for culture of non-adherent cells," *Sens. Actuators, B* **156**, 1002–1008 (2011).
- ⁶⁰M. Marimuthu and S. Kim, "Pumpless steady-flow microfluidic chip for cell culture," *Anal. Biochem.* **437**, 161–163 (2013).
- ⁶¹W. Gu, X. Zhu, N. Futai, B. S. Cho, and S. Takayama, "Computerized microfluidic cell culture using elastomeric channels and Braille displays," *Proc. Natl. Acad. Sci. U.S.A.* **101**, 15861–15866 (2004).
- ⁶²I. Barbulovic-Nad, S. H. Au, and A. R. Wheeler, "A microfluidic platform for complete mammalian cell culture," *Lab Chip* **10**, 1536–1542 (2010).

- ⁶³D. Bogojevic, M. D. Chamberlain, I. Barbulovic-Nad, and A. R. Wheeler, "A digital microfluidic method for multiplexed cell-based apoptosis assays," *Lab Chip* **12**, 627–634 (2012).
- ⁶⁴S. Srigunapalan, I. A. Eydelnant, C. A. Simmons, and A. R. Wheeler, "A digital microfluidic platform for primary cell culture and analysis," *Lab Chip* **12**, 369–375 (2012).
- ⁶⁵I. A. Eydelnant, U. Uddayasankar, B. Li, M. W. Liao, and A. R. Wheeler, "Virtual microwells for digital microfluidic reagent dispensing and cell culture," *Lab Chip* **12**, 750–757 (2012).
- ⁶⁶Y. C. Toh, T. C. Lim, D. Tai, G. Xiao, D. Van Noort, and H. Yu, "A microfluidic 3D hepatocyte chip for drug toxicity testing," *Lab Chip* **9**, 2026–2035 (2009).
- ⁶⁷C. C. Hsieh, S. B. Huang, P. C. Wu, D. B. Shieh, and G. B. Lee, "A microfluidic cell culture platform for real-time cellular imaging," *Biomed. Microdevices* **11**(4), 903–913 (2009).
- ⁶⁸S. B. Huang, S. S. Wang, C. H. Hsieh, Y. C. Lin, C. S. Lai, and M. H. Wu, "An integrated microfluidic cell culture system for high-throughput perfusion three-dimensional cell culture-based assays: Effect of cell culture model on the results of chemosensitivity assays," *Lab Chip* **13**, 1133–1143 (2013).
- ⁶⁹K. Ziólkowska, A. Stelmachowska, R. Kwapiszewski, M. Chudy, A. Dybko, and Z. Brzózka, "Long-term three-dimensional cell culture and anticancer drug activity evaluation in a microfluidic chip," *Biosens. Bioelectron.* **40**, 68–74 (2013).
- ⁷⁰K. Gupta, D. H. Kim, D. Ellison, C. Smith, A. Kundu, J. Tuan, K. Y. Suh, and A. Levchenko, "Lab-on-a-chip devices as an emerging platform for stem cell biology," *Lab Chip* **10**, 2019–2031 (2010).
- ⁷¹N. S. Hwang, S. Varghese, and J. Elisseeff, "Controlled differentiation of stem cells," *Adv. Drug Delivery Rev.* **60**, 199–214 (2008).
- ⁷²S. Mitalipov and D. Wolf, "Totipotency, pluripotency and nuclear reprogramming," *Adv. Biochem. Eng. Biotechnol.* **114**, 185–199 (2009).
- ⁷³K. I. Kamei, S. Guo, Z. T. F. Yu, H. Takahashi, E. Gschwend, C. Suh, X. Wang, J. Tang, J. McLaughlin, O. N. Witte, K. B. Lee, and H. R. Tseng, "An integrated microfluidic culture device for quantitative analysis of human embryonic stem cells," *Lab Chip* **9**, 555–563 (2009).
- ⁷⁴A. Khademhosseini, L. Ferreira, J. Blumling III, J. Yeh, J. M. Karp, J. Fukuda, and R. Langer, "Co-culture of human embryonic stem cells with murine embryonic fibroblasts on microwell-patterned substrates," *Biomaterials* **27**, 5968–5977 (2006).
- ⁷⁵J. C. Mohr, J. Zhang, S. M. Azarin, A. G. Soerens, J. J. de Pablo, J. A. Thomson, G. E. Lyons, S. P. Palecek, and T. J. Kamp, "The microwell control of embryoid body size in order to regulate cardiac differentiation of human embryonic stem cells," *Biomaterials* **31**, 1885–1893 (2010).
- ⁷⁶Y. S. Torisawa, B. H. Chueh, D. Huh, P. Ramamurthy, T. M. Roth, K. F. Barald, and S. Takayama, "Efficient formation of uniform-sized embryoid bodies using a compartmentalized microchannel device," *Lab Chip* **7**, 770–776 (2007).
- ⁷⁷M. Villa, S. Pope, J. Conover, and T. H. Fan, "Growth of primary embryo cells in a microculture system," *Biomed. Microdevices* **12**, 253–261 (2010).
- ⁷⁸M. Khoury, A. Bransky, N. Korin, L. C. Konak, G. Enikolopov, I. Tzchori, and S. Levenberg, "A microfluidic traps system supporting prolonged culture of human embryonic stem cells aggregates," *Biomed. Microdevices* **12**, 1001–1008 (2010).
- ⁷⁹C. L. Bauwens, R. Peerani, S. Niebruegge, K. A. Woodhouse, E. Kumacheva, M. Husain, and P. W. Zandstra, "Control of human embryonic stem cell colony and aggregate size heterogeneity influences differentiation trajectories," *Stem Cells* **26**, 2300–2310 (2008).
- ⁸⁰L. Kim, M. D. Vahey, H. Y. Lee, and J. Voldman, "Microfluidic arrays for logarithmically perfused embryonic stem cell culture," *Lab Chip* **6**, 394–406 (2006).
- ⁸¹J. Shi, L. Liu, and Y. Chen, "Investigation of cell culture in microfluidic devices with different bi-layer substrates," *Microelectron. Eng.* **88**, 1693–1697 (2011).
- ⁸²C. Kim, K. S. Lee, J. H. Bang, Y. E. Kim, M. C. Kim, K. W. Oh, S. H. Lee, and J. Y. Kang, "3-Dimensional cell culture for on-chip differentiation of stem cells in embryoid body," *Lab Chip* **11**, 874–882 (2011).
- ⁸³P. Aguiari, S. Leo, B. Zavan, V. Vindigni, A. Rimessi, K. Bianchi, C. Franzin, R. Cortivo, M. Rossato, R. Vettor, G. Abatangelo, T. Pozzan, P. Pinton, and R. Rizzuto, "High glucose induces adipogenic differentiation of muscle-derived stem cells," *Proc. Natl. Acad. Sci. U.S.A.* **105**, 1226–1231 (2008).
- ⁸⁴Z. Ivanovic, "Hypoxia or *in situ* normoxia: The stem cell paradigm," *J. Cell. Physiol.* **219**, 271–275 (2009).
- ⁸⁵Q. Zhang and R. H. Austin, "Applications of microfluidics in stem cell biology," *BioNanoScience* **2**, 277–286 (2012).
- ⁸⁶J. Dahlmann, G. Kensah, H. Kempf, D. Skvorc, A. Gawol, D. A. Elliott, G. Dräger, R. Zweigerdt, U. Martin, and I. Gruh, "The use of agarose microwells for scalable embryoid body formation and cardiac differentiation of human and murine pluripotent stem cells," *Biomaterials* **34**, 2463–2471 (2013).
- ⁸⁷L. G. Villa-Diaz, Y. S. Torisawa, T. Uchida, J. Ding, N. C. Nogueira-De-Souza, K. S. O'Shea, S. Takayama, and G. D. Smith, "Microfluidic culture of single human embryonic stem cell colonies," *Lab Chip* **9**, 1749–1755 (2009).
- ⁸⁸H. S. Shin, H. J. Kim, S. K. Min, S. H. Kim, B. M. Lee, and N. L. Jeon, "Compartmental culture of embryonic stem cell-derived neurons in microfluidic devices for use in axonal biology," *Biotechnol. Lett.* **32**, 1063–1070 (2010).
- ⁸⁹E. Cimetta, E. Figallo, C. Cannizzaro, N. Elvassore, and G. Vunjak-Novakovic, "Micro-bioreactor arrays for controlling cellular environments: Design principles for human embryonic stem cell applications," *Methods* **47**, 81–89 (2009).
- ⁹⁰X. Ju, D. Li, N. Gao, Q. Shi, and H. Hou, "Hepatogenic differentiation of mesenchymal stem cells using microfluidic chips," *Biotechnol. J.* **3**, 383–391 (2008).
- ⁹¹Y. Yang, K. Kulangara, J. Sia, L. Wang, and K. W. Leong, "Engineering of a microfluidic cell culture platform embedded with nanoscale features," *Lab Chip* **11**, 1638–1646 (2011).
- ⁹²A. C. Barbati, C. Fang, G. A. Banker, and B. J. Kirby, "Culture of primary rat hippocampal neurons: Design, analysis, and optimization of a microfluidic device for cell seeding, coherent growth, and solute delivery," *Biomed. Microdevices* **15**, 97–108 (2013).
- ⁹³H. W. Wu, X. Z. Lin, S. M. Hwang, and G. B. Lee, "The culture and differentiation of amniotic stem cells using a microfluidic system," *Biomed. Microdevices* **11**, 869–881 (2009).
- ⁹⁴R. Gómez-Sjöberg, A. A. Leyrat, D. M. Pirone, C. S. Chen, and S. R. Quake, "Versatile, fully automated, microfluidic cell culture system," *Anal. Chem.* **79**, 8557–8563 (2007).

- ⁹⁵J. B. Gurdon and P. Y. Bourillot, "Morphogen gradient interpretation," *Nature* **413**, 797–803 (2001).
- ⁹⁶H. L. Ashe and J. Briscoe, "The interpretation of morphogen gradients," *Development* **133**, 385–394 (2006).
- ⁹⁷D. Wu, "Signaling mechanisms for regulation of chemotaxis," *Cell Res.* **15**, 52–56 (2005).
- ⁹⁸L. Wang, D. Liu, B. Wang, J. Sun, and L. Li, "Design of parallel microfluidic gradient-generating networks for studying cellular response to chemical stimuli," *Front. Chem. China* **3**, 384–390 (2008).
- ⁹⁹J. Ruan, L. Wang, M. Xu, D. Cui, X. Zhou, and D. Liu, "Fabrication of a microfluidic chip containing dam, weirs and gradient generator for studying cellular response to chemical modulation," *Mater. Sci. Eng., C* **29**, 674–679 (2009).
- ¹⁰⁰G. N. Li, J. Liu, and D. Hoffman-Kim, "Multi-molecular gradients of permissive and inhibitory cues direct neurite outgrowth," *Ann. Biomed. Eng.* **36**, 889–904 (2008).
- ¹⁰¹C. J. Wang, X. Li, B. Lin, S. Shim, G. L. Ming, and A. Levchenko, "A microfluidics-based turning assay reveals complex growth cone responses to integrated gradients of substrate-bound ECM molecules and diffusible guidance cues," *Lab Chip* **8**, 227–237 (2008).
- ¹⁰²J. Y. Park, S. K. Kim, D. H. Woo, E. J. Lee, J. H. Kim, and S. H. Lee, "Differentiation of neural progenitor cells in a microfluidic chip-generated cytokine gradient," *Stem Cells* **27**, 2646–2654 (2009).
- ¹⁰³J. Y. Park, S. J. Yoo, C. M. Hwang, and S. H. Lee, "Simultaneous generation of chemical concentration and mechanical shear stress gradients using microfluidic osmotic flow comparable to interstitial flow," *Lab Chip* **9**, 2194–2202 (2009).
- ¹⁰⁴G. A. Cooksey, C. G. Sip, and A. Folch, "A multi-purpose microfluidic perfusion system with combinatorial choice of inputs, mixtures, gradient patterns, and flow rates," *Lab Chip* **9**, 417–426 (2009).
- ¹⁰⁵C. G. Sip, N. Bhattacharjee, and A. Folch, "A modular cell culture device for generating arrays of gradients using stacked microfluidic flows," *Biomicrofluidics* **5**(2), 022210 (2011).
- ¹⁰⁶E. Jedrych, S. Flis, K. Sofinska, Z. Jastrzebski, M. Chudy, A. Dybko, and Z. Brzozka, "Evaluation of cytotoxic effect of 5-fluorouracil on human carcinoma cells in microfluidic system," *Sens. Actuators, B* **160**, 1544–1551 (2011).
- ¹⁰⁷C. G. Yang, Y. F. Wu, Z. R. Xu, and J. H. Wang, "A radial microfluidic concentration gradient generator with high-density channels for cell apoptosis assay," *Lab Chip* **11**, 3305–3312 (2011).
- ¹⁰⁸E. Cimetta, C. Cannizzaro, R. James, T. Biechele, R. T. Moon, N. Elvassore, and G. Vunjak-Novakovic, "Microfluidic device generating stable concentration gradients for long term cell culture: Application to Wnt3a regulation of β -catenin signaling," *Lab Chip* **10**, 3277–3283 (2010).
- ¹⁰⁹L. J. Millet, M. E. Stewart, R. G. Nuzzo, and M. U. Gillette, "Guiding neuron development with planar surface gradients of substrate cues deposited using microfluidic devices," *Lab Chip* **10**, 1525–1535 (2010).
- ¹¹⁰N. Bhattacharjee, N. Li, T. M. Keenan, and A. Folch, "A neuron-benign microfluidic gradient generator for studying the response of mammalian neurons towards axon guidance factors," *Integr. Biol.* **2**, 669–679 (2010).
- ¹¹¹H. Wu, B. Huang, and R. N. Zare, "Generation of complex, static solution gradients in microfluidic channels," *J. Am. Chem. Soc.* **128**, 4194–4195 (2006).
- ¹¹²B. Mosadegh, C. Huango, J. W. Park, H. S. Shin, B. G. Chung, S. K. Hwang, K. H. Lee, H. J. Kim, J. Brody, and N. L. Jeon, "Generation of stable complex gradients across two-dimensional surfaces and three-dimensional gels," *Langmuir* **23**, 10910–10912 (2007).
- ¹¹³W. Saadi, S. W. Rhee, F. Lin, B. Vahidi, B. G. Chung, and N. L. Jeon, "Generation of stable concentration gradients in 2D and 3D environments using a microfluidic ladder chamber," *Biomed. Microdevices* **9**, 627–635 (2007).
- ¹¹⁴V. V. Abhyankar, M. W. Toepke, C. L. Cortesio, M. A. Lokuta, A. Huttenlocher, and D. J. Beebe, "A platform for assessing chemotactic migration within a spatiotemporally defined 3D microenvironment," *Lab Chip* **8**, 1507–1515 (2008).
- ¹¹⁵U. Haessler, Y. Kalinin, M. A. Swartz, and M. Wu, "An agarose-based microfluidic platform with a gradient buffer for 3D chemotaxis studies," *Biomed. Microdevices* **11**, 827–835 (2009).
- ¹¹⁶C. R. Kothapalli, E. Van Veen, S. De Valence, S. Chung, I. K. Zervantonakis, F. B. Gertler, and R. D. Kamm, "A high-throughput microfluidic assay to study neurite response to growth factor gradients," *Lab Chip* **11**, 497–507 (2011).
- ¹¹⁷Y. Shin, J. S. Jeon, S. Han, G. S. Jung, S. Shin, S. H. Lee, R. Sudo, R. D. Kamm, and S. Chung, "In vitro 3D collective sprouting angiogenesis under orchestrated ANG-1 and VEGF gradients," *Lab Chip* **11**, 2175–2181 (2011).
- ¹¹⁸J. Atencia, J. Morrow, and L. E. Locascio, "The microfluidic palette: A diffusive gradient generator with spatio-temporal control," *Lab Chip* **9**, 2707–2714 (2009).
- ¹¹⁹D. Kim, M. A. Lokuta, A. Huttenlocher, and D. J. Beebe, "Selective and tunable gradient device for cell culture and chemotaxis study," *Lab Chip* **9**, 1797–1800 (2009).
- ¹²⁰T. Kim, M. Pinelis, and M. M. Maharbiz, "Generating steep, shear-free gradients of small molecules for cell culture," *Biomed. Microdevices* **11**, 65–73 (2009).
- ¹²¹M. Kim and T. Kim, "Diffusion-based and long-range concentration gradients of multiple chemicals for bacterial chemotaxis assays," *Anal. Chem.* **82**, 9401–9409 (2010).
- ¹²²D. C. W. Tan, L. Y. L. Yung, and P. Roy, "Controlled microscale diffusion gradients in quiescent extracellular fluid," *Biomed. Microdevices* **12**, 523–532 (2010).
- ¹²³S. Kim, H. J. Kim, and N. L. Jeon, "Biological applications of microfluidic gradient devices," *Integr. Biol.* **2**, 584–603 (2010).
- ¹²⁴W. Dai, Y. Zheng, K. Q. Luo, and H. Wu, "A prototypic microfluidic platform generating stepwise concentration gradients for real-time study of cell apoptosis," *Biomicrofluidics* **4**(2), 024101 (2010).
- ¹²⁵Y. H. Jang, M. J. Hancock, S. B. Kim, S. Selimović, W. Y. Sim, H. Bae, and A. Khademhosseini, "An integrated microfluidic device for two-dimensional combinatorial dilution," *Lab Chip* **11**, 3277–3286 (2011).
- ¹²⁶Y. Shin, S. Han, J. S. Jeon, K. Yamamoto, I. K. Zervantonakis, R. Sudo, R. D. Kamm, and S. Chung, "Microfluidic assay for simultaneous culture of multiple cell types on surfaces or within hydrogels," *Nat. Protoc.* **7**, 1247–1259 (2012).
- ¹²⁷H. Jiang, W. Qu, Y. Li, W. Zhong, and W. Zhang, "Platelet-derived growth factors-bb and fibroblast growth factors-base induced proliferation of Schwann cells in a 3D environment," *Neurochem. Res.* **38**, 346–355 (2013).
- ¹²⁸E. Choi, I. Jun, H. K. Chang, K. M. Park, H. Shin, K. D. Park, and J. Park, "Quantitatively controlled *in situ* formation of hydrogel membranes in microchannels for generation of stable chemical gradients," *Lab Chip* **12**, 302–308 (2012).
- ¹²⁹Y. Ito, "Surface micropatterning to regulate cell functions," *Biomaterials* **20**, 2333–2342 (1999).

- ¹³⁰N. Patrito, C. McCague, P. R. Norton, and N. O. Petersen, "Spatially controlled cell adhesion via micropatterned surface modification of poly(dimethylsiloxane)," *Langmuir* **23**, 715–719 (2007).
- ¹³¹H. Yamazoe, T. Okuyama, H. Suzuki, and J. Fukuda, "Fabrication of patterned cell co-cultures on albumin-based substrate: Applications for microfluidic devices," *Acta Biomater.* **6**, 526–533 (2010).
- ¹³²V. Sivagnanam, B. Song, C. Vandevyver, J. C. G. Bünzli, and M. A. M. Gijs, "Selective breast cancer cell capture, culture, and immunocytochemical analysis using self-assembled magnetic bead patterns in a microfluidic chip," *Langmuir* **26**, 6091–6096 (2010).
- ¹³³E. Tenstad, A. Tourovskaia, A. Folch, O. Myklebost, and E. Rian, "Extensive adipogenic and osteogenic differentiation of patterned human mesenchymal stem cells in a microfluidic device," *Lab Chip* **10**, 1401–1409 (2010).
- ¹³⁴A. Khademhosseini, G. Eng, J. Yeh, P. A. Kucharczyk, R. Langer, G. Vunjak-Novakovic, and M. Radisic, "Microfluidic patterning for fabrication of contractile cardiac organoids," *Biomed. Microdevices* **9**, 149–157 (2007).
- ¹³⁵N. D. Dinh, Y. Y. Chiang, H. Hardelauf, J. Baumann, E. Jackson, S. Waide, J. Sisnaiske, J. P. Frimat, C. V. Thriell, D. Janasek, J. M. Peyrin, and J. West, "Microfluidic construction of minimalistic neuronal co-cultures," *Lab Chip* **13**, 1402–1412 (2013).
- ¹³⁶A. Kunze, M. Giugliano, A. Valero, and P. Renaud, "Micropatterning neural cell cultures in 3D with a multi-layered scaffold," *Biomaterials* **32**, 2088–2098 (2011).
- ¹³⁷R. I. Zeitoun, D. S. Chang, S. M. Langelier, J. Mirecki-Millunchick, M. J. Solomon, and M. A. Burns, "Selective arraying of complex particle patterns," *Lab Chip* **10**, 1142–1147 (2010).
- ¹³⁸B. Alp, J. S. Andrews, V. P. Mason, I. P. Thompson, R. Wolowacz, and G. H. Markx, "Building structured biomaterials using AC electrokinetics," *IEEE Eng. Med. Biol. Mag.* **22**, 91–97 (2003).
- ¹³⁹D. S. Gray, J. L. Tan, J. Voldman, and C. S. Chen, "Dielectrophoretic registration of living cells to a microelectrode array," *Biosens. Bioelectron.* **19**, 771–780 (2004).
- ¹⁴⁰M. Frénéa, S. P. Faure, B. Le Pioufle, P. Coquet, and H. Fujita, "Positioning living cells on a high-density electrode array by negative dielectrophoresis," *Mater. Sci. Eng., C* **23**, 597–603 (2003).
- ¹⁴¹Z. R. Gagnon, "Cellular dielectrophoresis: Applications to the characterization, manipulation, separation and patterning of cells," *Electrophoresis* **32**, 2466–2487 (2011).
- ¹⁴²C. T. Ho, R. Z. Lin, W. Y. Chang, H. Y. Chang, and C. H. Liu, "Rapid heterogeneous liver-cell on-chip patterning via the enhanced field-induced dielectrophoresis trap," *Lab Chip* **6**, 724–734 (2006).
- ¹⁴³K. Park, H. J. Suk, D. Akin, and R. Bashir, "Dielectrophoresis-based cell manipulation using electrodes on a reusable printed circuit board," *Lab Chip* **9**, 2224–2229 (2009).
- ¹⁴⁴M. Yang and X. Zhang, "Electrical assisted patterning of cardiac myocytes with controlled macroscopic anisotropy using a microfluidic dielectrophoresis chip," *Sens. Actuators, A* **135**, 73–79 (2007).
- ¹⁴⁵J. Schütte, B. Hagemeyer, F. Holzner, M. Kubon, S. Werner, C. Freudigmann, K. Benz, J. Böttger, R. Gebhardt, H. Becker, and M. Stelzle, "Artificial micro organs'-a microfluidic device for dielectrophoretic assembly of liver sinusoids," *Biomed. Microdevices* **13**(3), 493–501 (2011).
- ¹⁴⁶H. Wang, G. M. Riha, S. Yan, M. Li, H. Chai, H. Yang, Q. Yao, and C. Chen, "Shear stress induces endothelial differentiation from a murine embryonic mesenchymal progenitor cell line," *Arterioscler., Thromb., Vasc. Biol.* **25**, 1817–1823 (2005).